Bio-Design and Manufacturing (2025) 8:847–876
https://doi.org/10.1631/bdm.2400490

REVIEW

Microporous 3D bioprinting: a novel technology for biofabrication

Hongxiang Cai[1] · Yongrui Cai[1] · Zichuan Ding[1] · Jiaxuan Fan[1] · Yahao Lai[1] · Chao Huang[1] · Boyi Jiang[1] · Can Zhou[1] · Zongke Zhou[1] · Xingcai Zhang[2] · Zeyu Luo[1]

Received: 7 December 2024 / Accepted: 11 February 2025 / Published online: 6 September 2025

Abstract

Three-dimensional (3D) bioprinting provides a rapid and efficient method for fabricating customized bioprinted tissues that replicate the complex architecture of native tissues. However, in 3D bioprinting, the need for dense biomaterial networks to ensure mechanical strength and structural fidelity often restricts the spreading, migration, and proliferation of encapsulated cells, as well as the transport of materials. This review summarizes effective strategies for manufacturing microporous bioprinted tissues via 3D bioprinting. The term "microporous" refers to interconnected, micrometer-sized pore-like structures within the internal materials of bioprinted tissues, including the microstructure of a single extruded fiber in extrusion printing. This differs from the macroscopic pore structure formed between fibers composed of print tracks or computer-aided design presets. These micropores play a crucial role in advancing biomanufacturing and 3D bioprinting by providing space for cell adhesion and proliferation while facilitating the timely transport of nutrients and metabolic waste essential for cell growth. Additionally, microporous bioprinted tissues offer the mechanical support needed for cell seeding and serve as sites for extracellular matrix deposition. As microporous 3D bioprinting continues to advance, it has the potential to address unresolved challenges in fields such as organ transplantation, tissue regeneration, and tissue replacement.

Hongxiang Cai and Yongrui Cai have contributed equally to this work.

✉ Zongke Zhou
Zhouzongke@scu.edu.cn

✉ Xingcai Zhang
drzhangxingcai@outlook.com

✉ Zeyu Luo
luozy@wchscu.edu.cn

[1] Orthopaedic Research Institute, Department of Orthopaedics, West China Hospital, Sichuan University, Chengdu 610041, China

[2] World Tea Organization, Cambridge, MA 02139, USA

Graphical abstract

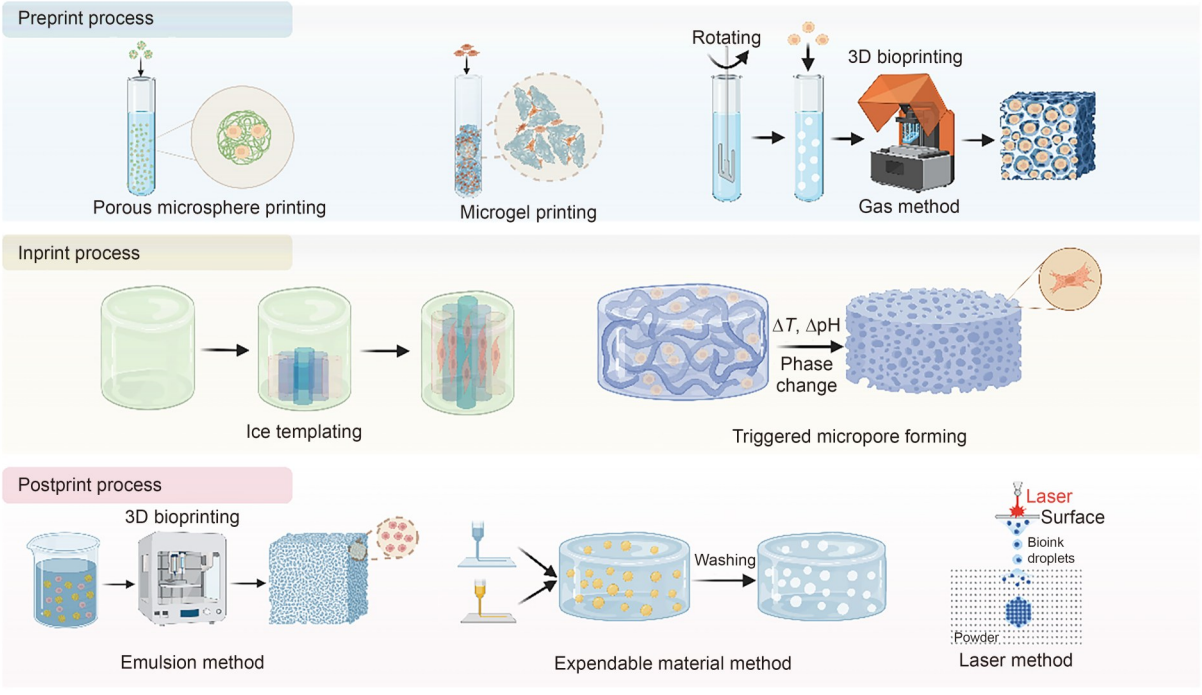

Keywords Bioprinting · Microporous · Hydrogel · Biofabrication

1 Introduction

Over the past two decades, the limitations of classical tissue engineering in fabricating complex bionic structures have led to the oversimplification of tissue architectures, resulting in engineered tissues that fail to replicate realistic cellular microenvironments. Three-dimensional (3D) bioprinting, with its ability to fabricate intricate and biomimetic tissue structures, offers a promising solution to this challenge [1]. 3D bioprinting involves converting bioinks containing living cells into functional tissue structures and organs based on 3D digital models. This technology has demonstrated potential for generating tissues and organs suitable for various biomedical applications, including transplantation and drug screening [2]. Bioprinting technology has evolved from droplet, extrusion, stereolithography apparatus (SLA), and digital light processing (DLP) to volumetric and, more recently, ultrasound bioprinting [3]. Different bioprinting techniques also require specific bioink properties. Droplet bioprinting necessitates low-viscosity bioinks [4], while extrusion bioprinting relies on shear-thinning bioinks [5]. DLP bioprinting requires photo-curable bioinks with moderate viscosity [6], volumetric bioprinting depends on bioinks with high light transmittance [7], and ultrasound bioprinting requires acoustically responsive bioinks [8]. Key characteristics of an ideal bioink include bioprintability, high mechanical integrity and stability, insolubility in cell culture medium, biodegradability suitable for tissue regeneration, nontoxicity, nonimmunogenicity, and the ability to promote cell adhesion [9]. Furthermore, bioinks should be easy to manufacture and process, cost-effective, and commercially available [10]. Two primary types of bioinks are used in 3D bioprinting of tissues and organs. The first and most common type is scaffold-based bioink, in which cells are embedded within hydrogels or similar exogenous materials before being bioprinted into 3D structures. Examples include agarose [11], alginate [12], chitosan [13], collagen type I [14], fibrin [15], gelatin [16], hyaluronic acid [17], and methacrylated gelatin [18]. These cell-laden hydrogels support cell proliferation and growth, facilitating tissue formation [19–21]. The second type is scaffold-free bioink, which does not rely on exogenous biomaterials. Instead, cells are bioprinted using a scaffold-free approach that mimics embryonic development. Examples include tissue spheroids [22], cell pellets [23], and tissue strands [24]. In this process, cells first form pre-structured tissues, which are then used for bioprinting [25]. The printed tissues are deposited in a specific pattern, allowing them to fuse and mature into functional tissues on a larger scale [26]. Scaffold-free bioinks enhance cell growth, proliferation, and diffusion, enabling better integration with surrounding tissues.

Advancements in bioprinting technology and bioink development continue to address the challenges of conventional tissue engineering, offering more effective solutions for tissue regeneration [27].

The demanding physiological conditions of the human body impose stringent requirements on the performance of bioprinted tissues. First, these tissues must exhibit mechanical properties comparable to those of the implantation site to ensure stability during healing and degradation [28, 29]. Second, they must possess appropriate biological properties, including long-term cell survival, migration, osmosis, and substance exchange, all of which are essential for maintaining structural integrity and biological function [30, 31]. Current 3D bioprinting techniques remain limited, as they primarily focus on the initial state of the printed object, assuming it to be static and inanimate. This approach fails to achieve an optimal balance between the biological and mechanical properties of bioprinted tissues [32]. Additionally, inaccuracy in the shape of bioprinted constructs presents a significant clinical challenge, particularly for bone designs requiring high-resolution precision [33]. Microporous 3D bioprinting has been developed to address these limitations by introducing micropores that balance the physical and biological properties of bioprinted tissues. This technique enhances cell survival, migration, infiltration, and material exchange in vivo. Multiscale porosity is essential for this process and includes the following pore types [34]: (1) macroscopic pores/channels (⩾1 mm), which facilitate nutrient transport, similar to vascular networks, though insufficient for supporting tissue-like structures; (2) mesoscale pores (100 μm–1 mm), which promote nutrient diffusion and slow degradation, supporting new tissue formation; (3) micropores (1–100 μm), providing structural support and facilitating nutrient uptake and retention; (4) nanopores (<100 nm), serving as pathways for small molecules such as proteins and nutrients. However, most 3D bioprinting studies rely on dense bioinks with low porosity to preserve mechanical strength and structural integrity. This design choice results in inadequate nutrient and oxygen diffusion, ultimately hindering cell migration and proliferation [35–39]. The fabrication of bioprinted tissues with multiscale porous networks is crucial for efficient nutrient and oxygen diffusion, as well as cellular support, facilitating the development of functional tissues. Porous hydrogel-based bioprinted tissues offer significant advantages over nonporous ones in 3D cell culture [40]. For instance, Gupta et al. [41] fabricated complex-shaped gelatin–gellan composite bioprinted tissues with multiscale porosity for bone tissue regeneration using a combination of low-temperature 3D printing and lyophilization. Their findings revealed that multiscale porous bioprinted tissues surpassed those with only micropores and macropores in swelling rate, degradation rate, pore distribution uniformity, cell infiltration, attachment, proliferation, protein production, and mineralization. These results indicated that multiscale porosity enhanced cell permeation, retention, viability, proliferation, and the functional generation of extracellular matrix.

In this review, we summarize microporous bioprinting methods, categorizing them into preprint, inprint, and postprint processing (Fig. 1). Preprint processing involves generating microporous structures before bioprinting. Key approaches include the porous microsphere method, the microgel method, and the gas method. The porous microsphere method is a hybrid 3D bioprinting technique that integrates porous bioprinted tissues with extrusion printing, utilizing cell-laden bioprinted tissues and polymeric microcarriers such as microspheres. This method enhanced cell adhesion and proliferation prior to printing, combining traditional bioprinting with advanced 3D technologies for tissue replacement and biological modeling [42, 43]. The microgel method employed annealed microgels to improve porosity and modularity, offering an alternative to conventional bioinks with superior rheological properties for printing diverse structures [44]. In this approach, cells were located within the pores between microgel particles, where they typically adhered to the microgel surface. The gas method, inspired by whipped cream production, generated hydrogel foam bioinks with multiscale, interconnected pores ranging from micrometers to several hundred micrometers [45]. Inprint processing refers to pore formation during the printing process, including cryobioprinting and triggered micropore formation. Cryobioprinting employed cryoprotected bioinks and a temperature-controlled freezing plate to produce vertical, high-aspect-ratio, cell-laden hydrogel structures with interconnected, anisotropic, gradient microchannels [46]. Triggered micropore formation used microphase separation, induced by stimuli such as body temperature or pH, to create highly interconnected, cell-sized pores [47]. Postprint processing refers to the formation of microporosity after bioprinting. The emulsion method was a cell-friendly approach for directly bioprinting microporous hydrogel structures using aqueous phase emulsion bioinks, which consist of single or dual aqueous phases or include an oil phase [48, 49]. The expendable material method involved depositing template and matrix bioinks layer by layer, followed by the removal of the template phase to create a network of interconnected tubular channels [50]. Sacrificial templates included materials such as sugar particles, salt crystals, or bacteria. Additional postprint processing techniques included femtosecond laser processing, microalgae-based methods, and recrystallization techniques. Furthermore, this review discusses the biological background and current challenges of each application, paving the way for the advancement of microporous bioprinting technology. Finally, we summarize the key challenges in microporous 3D bioprinting and outline future directions for its applications.

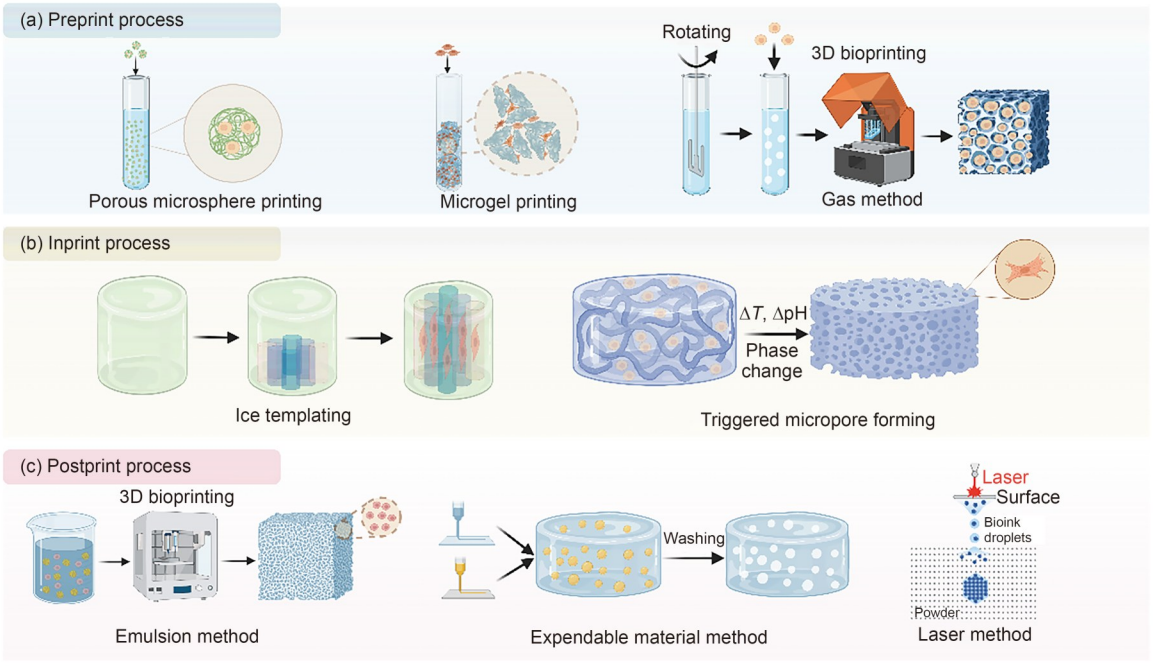

Fig. 1 Methods of microporous 3D bioprinting: (a) preprint process; (b) inprint process; (c) postprint process. Created in BioRender. Luo, Z. (2025) https://BioRender.com/nom1r6v

2 Fabrication method

2.1 Preprint processing

2.1.1 Porous microsphere printing

Conventional bioinks consisted of continuous hydrogel prepolymers that served as direct cell carriers, forming a dense network. To address this limitation, researchers modified or introduced additional cell carriers to create internal porous structures that supported cell survival, with porous microspheres exemplifying this approach [51]. Tan et al. [52] developed bioinks consisting of cell-laden poly(D,L-lactic-hydroxyacetic acid) (PLGA) porous microspheres encapsulated in agarose–collagen (AC) composite hydrogels. The highly porous microspheres provided a large surface area for cell attachment, infiltration, and growth before printing. Cells were seeded onto the microspheres, allowing them to infiltrate and proliferate, forming cell-loaded microspheres (CLMs). These CLMs were then coated with a thin layer of thermoresponsive AC hydrogel for bioprinting on a chilled platform, where agarose gelation occurred. Collagen fibrils formed after culturing the construct at 37 °C (Fig. 2a). The hydrogel acted as a lubricant during printing, while the addition of type I collagen enhanced cell adhesion. Micropipette printing facilitated compact packing. The results demonstrated successful printing of various cell types, with high viability and proliferation postprinting. Biocompatibility was excellent, with cell survival rates exceeding 90% after 2, 7, and 14 d. Additionally, the construct's mechanical strength improved by over 100-fold compared to AC hydrogel alone.

This method improved stacking capabilities for fabricating 3D structures compared to pure hydrogel bioprinting [53]. Volumetric 3D tissues were constructed in multiple layers. During extrusion printing, microspheres provided a cushioning or shielding effect, minimizing cell damage caused by shear stress. The printed structures created a conducive 3D environment for various cell types. Additionally, highly porous microscaffolds facilitated the loading of high-density cells more effectively than solid scaffolds, promoting accelerated degradation after printing. Using cell-loaded microscaffolds for 3D bioprinting required lower initial cell densities than conventional cell-loaded hydrogels or tissue spheres [51]. The selection of microsphere sizes was influenced by the trade-off between print resolution and cell density, with smaller microspheres enabling higher resolution. However, a limitation of this method was that the resolution and speed of extrusion-based printing remained insufficient for large-scale tissue fabrication [52].

In recent years, various 3D bioprinting techniques based on the microsphere method have been developed and broadly categorized into two types: extrusion bioprinting and DLP-based 3D bioprinting [54, 55]. Extrusion bioprinting methods, including nozzle extrusion and inkjet printing, selectively deposit bioinks at specified locations to construct 3D structures. However, due to physical constraints of the nozzle or inkjet head, the highest achievable resolution was typically approximately 50 μm [54]. In contrast,

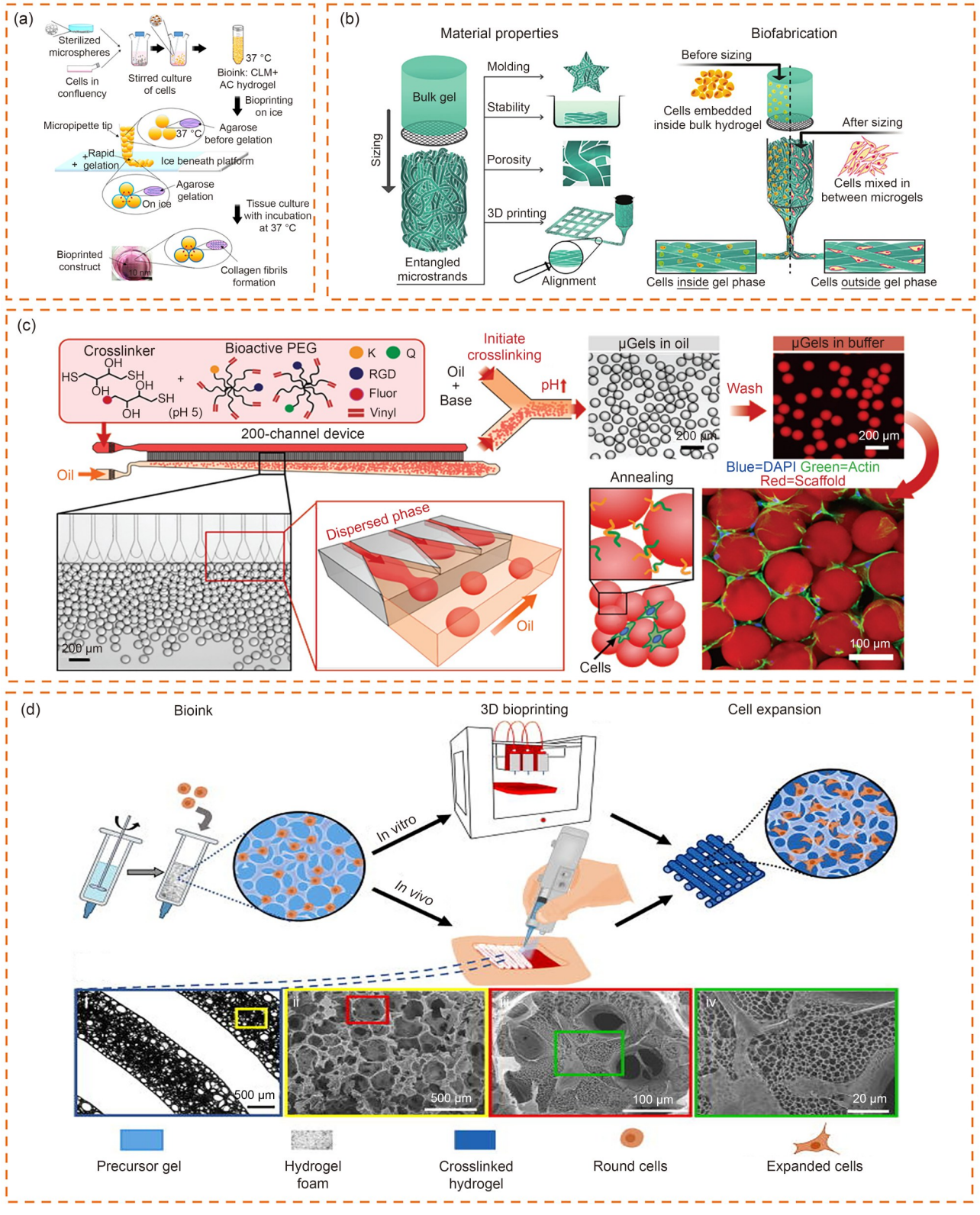

Fig. 2 Preprint processing. (a) Schematic representation of porous microsphere printing. Reproduced from [52], Copyright 2016, with permission from the authors, licensed under CC BY 4.0. (b) Bulk hydrogel was mechanically extruded through a grid to deconstruct it into microstrands, forming a bioink by embedding cells within the bulk hydrogel. Reproduced from [71], Copyright 2020, with permission from the authors, licensed under CC BY. (c) Overview of microgel production and in situ scaffold formation. Reproduced from [68], Copyright 2019, with permission from WILEY-VCH Verlag GmbH & Co. KGaA, Weinheim. (d) Method for engineering an adhesive foam bioink for 3D bioprinting, inspired by whipped cream formation. Reproduced from [45], Copyright 2021, with permission from AIP Publishing

DLP-based bioprinting selectively delivers photon energy to targeted locations, crosslinking (curing) biological materials to fabricate 3D structures. Because light could be precisely manipulated through optical lenses without being constrained by a physical aperture, DLP-based methods achieved resolutions on the micrometer or even submicrometer scale [56, 57]. However, the resolution of DLP-based bioprinting was affected by increased light scattering due to high cell densities in the bioink. To address this issue, You et al. [58] developed a method to mitigate resolution deterioration by incorporating iodixanol into the bioink, reducing light scattering tenfold and significantly improving resolution in high-cell-density (HCD) bioinks. For bioinks with a cell density of 100 million cells per milliliter, a fabrication resolution of 50 μm was achieved. To demonstrate its potential for 3D tissue and organ bioprinting, they fabricated thick HCD tissue with a fine vascular network. The tissue remained viable in a perfusion culture system, with endothelialization and angiogenesis observed after 14 d.

Porous microsphere printing integrates the advantages of solid scaffolds with emerging bio-3D printing techniques, enabling the fabrication of multiscale, multicellular 3D tissue structures. This approach represents a promising strategy for clinically relevant tissue replacement and the bioprinting of functional in vitro biological models. Additionally, direct cell bioprinting using spherocyte aggregates as bioinks has advanced the engineering of scaffold-free vascular tissues, functional organ modules, and cancer models [59]. Deo et al. [60] developed a biphasic microsphere bioink composed of cell-loaded polyethylene glycol (PEG) hydrogel particles embedded in a continuous gelatin methacryloyl (GelMA)-nanosilicate colloidal network. β-islet cells and endothelial cells were incorporated into the GelMA-nanosilicate colloidal network within PEG micro-particles. The results demonstrated that this biphasic bioink exhibited excellent rheological properties, high print fidelity, and structural stability. Furthermore, the microsphere method effectively facilitated the construction of complex tissue structures containing multiple cell types and heterogeneous microenvironments [60].

2.1.2 Microgel method

Microgels have emerged as biomaterials with distinct properties, including injectability for controlled flow, inherent porosity for structural filling, mechanical support through interparticle crosslinking, and modularity. Their macroporous structure has demonstrated significant potential in tissue repair by enhancing cell migration and infiltration both in vitro and in vivo [61, 62]. Granular hydrogels have also been modified to incorporate growth factors that induce chemotaxis for cellular infiltration or chemically altered to present bioadhesion sites, improving cell migration and behavior [63, 64]. Furthermore, they have been widely utilized as in vitro platforms for studying biological processes such as angiogenesis, cellular outgrowth, and cell condensation by integrating individual spheres or cell suspensions into their pores [65, 66].

Microgel scaffolds represent a novel approach in biomaterials for accelerating tissue regeneration in the skin, brain, and heart, as well as for studying cancer onset and progression. Microgels, derived from various biomaterials such as PEG, chitosan, alginate, gelatin, and acrylic polymers, have been investigated for use in bioinks, sphere fabrication, and stimulus-responsive structures [67]. Additionally, these modular particulate "inks" are compatible with 3D bioprinting technology and enable the formation of complex macrostructures with intrinsic microscopic pores, which improve nutrient and waste transport while facilitating immediate cellular infiltration [68].

Microgel bioinks offer the advantage of reduced inherent flow behavior compared to liquid bioinks. These bioinks exhibited shear-thinning and shear-recovery properties due to weak particle–particle interactions, which were disrupted by high shear stresses during nozzle extrusion and reformed postprinting [44]. When microgels were compressed into a close-packed state, they demonstrated moderate printability. The inherent gaps between microgels in this state allowed for higher cell viability, spreading, and migration compared to large monolithic materials [68] (Fig. 2c). Despite these advantages, the microgel method had several limitations, including poor scalability, the need for additives such as oils, and restrictions to low-viscosity polymer solutions [69]. Another limitation of this method was the spherical nature of the microgel, as the tightly packed mesh restricted interactions between individual spheres and prevented anisotropy in the printed material. Consequently, existing microgel bioinks required secondary crosslinking for stability in aqueous media and failed to provide essential guidance cues for aligning cells in anisotropic tissues, such as muscles and tendons [70]. Kessel et al. [71] demonstrated a simple and effective approach in which pre-crosslinked bulk hydrogels were broken down into microchains using a grid with a pore size of 40–100 μm. During extrusion, these microchains aligned, promoting myotube organization. The aligned hydrogel chains served as effective cues, enabling embedded cells to form oriented microtubules (Fig. 2b). Their method produced large quantities of high-aspect-ratio microgels and addressed many disadvantages associated with spherical microgel materials.

2.1.3 Gas method

The gas method is a technique for introducing interconnected multiscale pores into hydrogel networks, utilizing hydrogel foam bioinks for scaffold bioprinting. Through crosslinking, printed structures formed multiscale, interconnected

porous networks with pore sizes ranging from a few micrometers to several hundred micrometers [72]. Mostafavi et al. [45] developed a viscous foam bioink for 3D bioprinting, inspired by the formation of whipped cream. They first stirred a GelMA prepolymer solution at high speed using a homogenizer to create foam, then added 1% polyvinyl alcohol (PVA), a synthetic biocompatible polymer, as a surfactant. After foaming, they mixed cells with the GelMA foam bioink and printed the structures using either a 3D fixer or a handheld bioprinter. The in vitro and in vivo biocompatibility of the foam bioink was evaluated through subcutaneous implantation in rats, with monitoring over four weeks. After one week of implantation, all foam structures were fully occupied by cells that had infiltrated the scaffolds, and a significant number of microvessels were observed in both the foam scaffolds and surrounding tissues. In contrast, only minimal cellular infiltration was observed in most hydrogel samples. After four weeks of implantation, the foam had completely degraded and was replaced by new tissue, whereas the hydrogel sample remained intact as a scaffold within the subcutaneous tissue. These findings demonstrated that multiscale interconnected pores in foams significantly enhanced cellular infiltration, vascularization, and tissue regeneration (Fig. 2d). Weber et al. [73] further demonstrated the integration of a DLP printing process with a microfluidic chip system to generate size-tunable pores with narrow pore size distributions in a GelMA hydrogel matrix. This method enabled precise control over bubble formation within GelMA hydrogel precursors, allowing for tunable pore sizes. The cytocompatibility of the printed porous scaffolds was evaluated using fibroblasts, confirming high cell viability, as well as increased cell proliferation, spreading, and migration.

In this approach, pore size was controlled by adjusting the mixing time, mixing speed, and hydrogel concentration. Rheological analysis of foam and hydrogel bioinks revealed that foams exhibited smaller modulus changes and higher viscosity during the sol−gel transition compared to hydrogels, resulting in more stable and reproducible bioprinting parameters [45]. Due to these favorable mechanical and rheological properties, this method was also suitable for handheld printing devices [74]. Foam bioinks have applications in regenerative medicine, including skin, bone, and blood vessel repair [45, 74, 75]. Foam scaffolds facilitated scaffold remodeling by cells, promoting the formation of aligned fibers within the injured area. This adaptability allowed scaffolds to conform to shape defects, eliminating the need for sutures. Mainardi et al. [76] demonstrated that the gas method could produce macroscopic bioactive materials with complex 3D geometries, serving as a platform for novel bioprocessing applications. Additionally, foam bioinks exhibited strong adhesion to skin tissues, offering enhanced flexibility, ductility, shape fidelity, and structural stability, as well as improved adhesion to surrounding tissues in in vitro and ex vivo studies [77]. These foam scaffolds supported cellular activity and facilitated tissue integration by enhancing cellular infiltration and nutrient/waste transport. This, in turn, accelerated scaffold integration, vascularization, and innervation [78, 79]. However, the method required significant material input, as only certain materials—primarily protein-based—were suitable for constructing stable foam hydrogels, limiting its broader applicability [45].

2.2 Inprint processing

2.2.1 Cryobioprinting

Traditional 3D extrusion bioprinting has been the most widely used technology for constructing volumetric structures layer by layer over the past few decades [80]. Although effective in many applications, these methods have limitations in fabricating anisotropic tissues, such as muscle and nerve fibers, which require precise cellular alignment for proper physiological function [69]. Zhu et al. [81] developed extracellular matrix scaffolds with parallel microchannels by implanting sacrificial templates subcutaneously, followed by their removal and subsequent decellularization. These scaffolds exhibited exceptional versatility and flexibility, enabling the regeneration of vascularized and innervated neo-muscle, vascularized nerves, and pulsatile arteries with functional integration. This study underscored the critical role of cellular arrangement in the functionality of anisotropic tissues. Numerous studies have demonstrated that ice templating is a widely used technique for fabricating anisotropic materials with microchannels. The pore morphology was controlled by directing the formation of oriented ice in solute suspensions [82, 83]. During freezing, ice crystals formed in the biomaterial solution and propagated in a fixed direction. Upon crosslinking and thawing, the ice crystals melted, leaving behind interconnected anisotropic microchannels within the scaffold. Luo et al. [46] developed a vertical 3D cryobioprinting technology that integrated extrusion bioprinting, directed freezing, and cryopreservation. GelMA-based hydrogel scaffolds containing anisotropic microchannels were fabricated using ice templating (Fig. 3a). This technique successfully produced column arrays, angled filaments, multimaterial filaments, and scaffolds with heterogeneous filament arrays (Fig. 3b). Their results demonstrated that bioinks composed of GelMA and a cryoprotective agent were effective for vertical 3D cryobioprinting, achieving high cell encapsulation viability. Directional freezing facilitated the formation of interconnected, anisotropic, and gradient microchannels, promoting the directional alignment of cells (Fig. 3c). Skeletal myoblasts embedded in 3D frozen bioprinted hydrogel structures exhibited greater viability, spreading, and alignment compared to those in standard hydrogel structures.

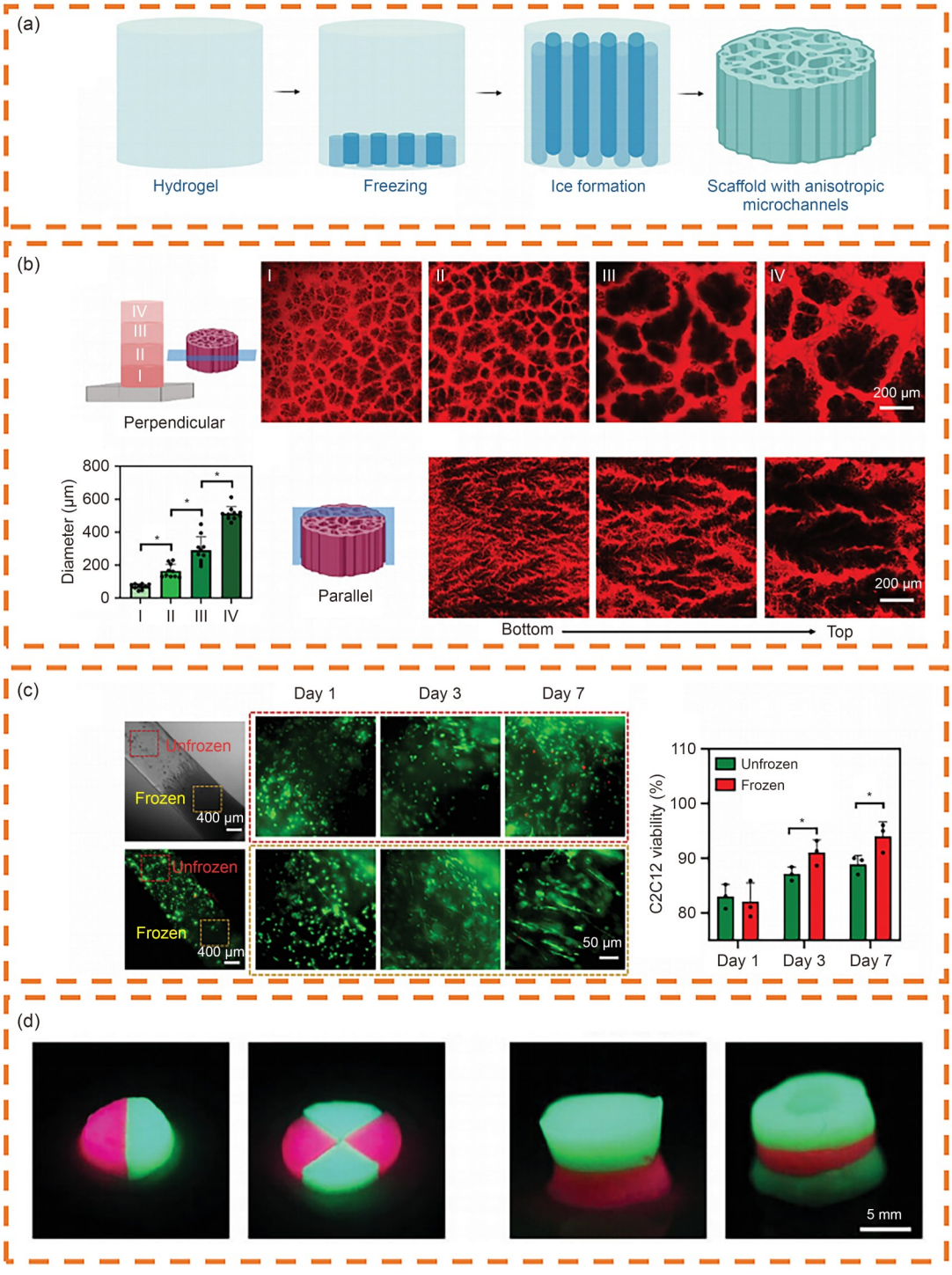

Fig. 3 Inprint processing. (a) GelMA-based hydrogels subjected to directional freezing formed interconnected, gradient, and anisotropic microchannels along the vertical axis. (b) Characterization of vertically ice-templated 7.5% GelMA constructs. (c) Behavioral analysis of C2C12 cells encapsulated in vertically cryobioprinted GelMA constructs. Reproduced from [46], Copyright 2022, with permission from Wiley-VCH GmbH. (d) Frozen modular GelMA scaffolds were easily assembled through photocrosslinking. Reproduced from [88], Copyright 2023, with permission from Wiley-VCH GmbH

Wu et al. [84] fabricated dressing scaffolds with a spatial design using chitosan as the matrix and bioglass as a biocomponent, employing a custom cryoprinting system. Their findings indicated that the printed scaffolds exhibited an interconnected, hierarchical pore structure with good flexibility and water absorption. Additionally, the micro- and macrostructures were highly controllable and reproducible, and these properties remained unaffected by bioglass content.

However, this technology has certain limitations. For instance, the print height was insufficient for some in vivo applications, necessitating further research. Additionally, cryobioprinting was integrated with 3D printing to create porous scaffolds. However, this approach was suboptimal for bioprinting, as cells needed to be seeded post-scaffold formation to avoid cold exposure, often resulting in low seeding density and uneven cell distribution, particularly in scaffolds with small pore sizes [85]. To enhance cell viability during and after the ice templating process, incorporating biomaterials with cryoprotective agents (CPAs) was essential. Dimethyl sulfoxide (DMSO) was one of the most commonly used CPAs, as it minimized cell membrane damage at low temperatures by preventing intracellular and extracellular ice crystallization [86]. Saccharides were also widely used as naturally derived CPAs. Due to their high molecular weight, saccharides could not penetrate cell membranes and instead acted on the extracellular surface. Furthermore, they reduced water contact with cells by increasing the osmotic pressure of the extracellular medium. Among disaccharides, melezitose exhibited excellent cryoprotective effects [87].

Cryobioprinting has demonstrated enhanced robustness and versatility, particularly in designing anisotropic tissues. This technology holds promise for various applications, including tissue engineering, regenerative medicine, drug discovery, and personalized therapy. Additionally, it can be adapted to multimaterial formats to explore potential applications, such as fabricating muscle-tendon and muscle-microvascular units. Wu et al. [84] utilized this method to prepare scaffolds with high fidelity, hierarchical porosity, and softness, making them effective as wound dressings for skin regeneration. Luo et al. [88] further optimized 3D cryoprinting by developing a strategy that assembled cryoprinted modular structures. In this approach, bioinks loaded with cells were extruded onto customized cryopanels to form 3D cryobioprinted modular scaffolds with customizable structures and functions. After recovery and crosslinking, these modular structures—featuring uniform or varied compositions—were assembled on-site, either in vitro or in vivo (Fig. 3d). This approach addressed major limitations of cryobioprinting by enabling scalable tissue fabrication through modular assembly. It also facilitated the creation of tissue structures from identical or different materials, allowing for precise reconstruction of defects of various sizes and shapes.

2.2.2 Triggered micropore forming

Research on cell and tissue structure suggests that porous, viscoelastic scaffolds that mimic host tissues can enhance the function of both native and transplanted cells, improving therapeutic outcomes [89]. However, simultaneously bioprinting cell-loaded scaffolds with cell-sized pores and a viscoelastic response remains challenging. Bao et al. [47] developed a bioprinting approach called "triggered micropore-forming" (TMF), which utilized a microphase separation mechanism activated by a slight stimulus to generate highly interconnected, cell-sized pores in a controlled manner. In this method, chitosan served as the bioink system, while cytocompatible PEG functioned as a crosslinking spacer, competing with chitosan to modulate hydrogen bond strength. First, the phase separation induction matrix (PSIM) was created by mixing sodium bicarbonate with a gelatin slurry. Bioinks embedded in PSIM were then 3D-printed to incorporate cells. Upon extrusion, the bioink reacted with sodium bicarbonate in PSIM, triggering a pH shift that induced a bicontinuous microphase of water and chitosan [90]. This reaction resulted in the formation of pores and a concentrated chitosan phase. The bioprinted porous viscoelastic hydrogel (PVH) scaffolds were stabilized at 37 °C, after which PSIM was removed. The results demonstrated that scaffolds produced using this method exhibited viscoelasticity comparable to biological tissues, with tunable porosity and stiffness. Despite their high porosity, the bioprinted scaffolds maintained excellent mechanical robustness. Additionally, the bioprinting method and the resulting scaffolds supported cell spreading, migration, and proliferation [47]. Dong et al. [91] introduced a method that combined 3D printing with DLP and polymerization-induced phase separation to fabricate 3D polymer structures with digitally defined geometries and controllable submicron-scale porosity. This approach produced 3D polymer structures with complex geometries and spatially controlled apertures ranging from 10 nm to 1000 μm. By enabling the fabrication of hierarchically porous 3D objects with structural features ranging from 10 nm to the centimeter scale, this method expanded the capabilities of 3D printing [92]. Compared to TMF, the polymerization-induced phase separation method provided finer control over pore size while promoting cell adhesion and the rapid growth of adherent cells. Bobrin et al. [93] developed an efficient and versatile process to fabricate 3D-printed materials with controllable nanoscale features. This method utilized resins containing macromolecular chain transfer agents (macroCTAs) to form nanostructured materials through microphase separation during light-induced 3D printing. By adjusting the macroCTA chain length, they achieved precise control over microphase separation, resulting in well-defined nanoscale size and morphology. Compared to TMF, this microphase separation approach enabled the fabrication of high-resolution multiscale structures, allowing for the fine-tuning of the overall mechanical properties of the 3D-printed object. This work demonstrated significant potential for fabricating layered structural materials for medical, engineering, and energy applications [93].

The TMF bioprinting method integrates embedded bioprinting, microphase separation, and viscoelastic hydrogels, offering several advantages. Microphase separation mitigated

nozzle clogging and structural collapse while enabling the use of low-viscosity bioinks, thereby reducing shear-induced cell damage during extrusion [94]. A key advantage of the TMF method was its ability to rapidly fabricate uniformly layered, cell-loaded hydrogels. Despite containing macroscopic (100 μm), microscopic (approximately 20 μm), and nanoscale (<100 nm) pores, TMF-prepared scaffolds exhibited remarkable mechanical toughness due to the concentration effect of microphase separation, a characteristic not observed in other bioprinting systems. Another significant advantage was the ability to independently adjust viscoelasticity, stiffness, and porosity through design modifications. This was achieved by adjusting pH levels and incorporating PEG. Additionally, TMF-prepared bioprinted scaffolds fully supported cell growth and migration with minimal physical constraints [95]. However, cell survival during pore induction may have been compromised, resulting in inefficient cell seeding and uneven distribution. Additionally, research on this method remained limited, and its potential applications required further exploration. Bao et al. [47] fabricated bilayer vocal fold structures by mixing human vocal fold fibroblasts with 0.02% collagen monomers. They then seeded human bronchial epithelial cells onto the basement membrane, forming a dense, connected epithelial layer on the construct's surface. This porous structure significantly enhanced fibroblast spreading compared to nonporous hydrogels. Furthermore, the hydrogel maintained structural integrity during coculture, demonstrating the feasibility of TMF bioprinting for creating pre-shaped, cell-laden scaffolds for coculture applications. Additionally, Bao et al. [47] bioprinted breast cancer cells into PVHs for in vitro cancer modeling. The PVH structure promoted cancer cell proliferation more effectively than nanoporous elastic hydrogel structures, confirming the compatibility of TMF bioprinting with cancer cells.

2.3 Postprint processing

2.3.1 Emulsion method

The successful fabrication of large-pore hydrogel structures via 3D bioprinting is often hindered by nozzle blockages caused by large particles, particularly in extrusion bioprinting. The emulsion method offers a promising strategy for generating microporous scaffolds by simultaneously printing two immiscible phases (Table 1). This approach enables precise control over porosity and interconnectivity by adjusting the composition, viscosity, and concentration of the emulsion ink [104]. The emulsion method involves either two aqueous phases or a combination of an aqueous and an oil phase (water-in-oil (w/o) or water-in-water (w/w)).

The w/o method utilizes an emulsion-based bioink consisting of an aqueous phase and an oil phase. By adjusting the mixing ratio of these components, hydrogels with varying pore sizes and porosities can be produced [111] (Fig. 4a). Kim and Kim [48] developed an emulsion-based bioink composed of methacrylated collagen (CMA) and mineral oil (MO) loaded with human adipose-derived stem cells (hASCs). In this biphasic colloidal system, the oil emulsion phase was formed by dispersing MO in a hydrophilic CMA solution, which was then uniformly distributed within a continuous aqueous phase. Their results demonstrated that cell proliferation and cytoskeletal reorganization were significantly enhanced in cellular structures printed with emulsion bioinks compared to those fabricated using conventional bioinks. Additionally, controlled release of bioactive molecules within these structures significantly promoted the chondrogenic and osteogenic differentiation of hASCs, as indicated by the expression of relevant genes. However, w/o methods often involve organic phases or surfactants, which can be cytotoxic. The w/w method addresses this limitation by eliminating biotoxicity while retaining the advantages of the w/o approach [109, 110, 112].

The w/w method forms an emulsion by mixing two incompatible hydrophilic biomaterials in an aqueous solution. Due to the thermodynamic incompatibility of certain water-soluble polymers, w/w emulsions do not require organic solvents, distinguishing them from conventional emulsion inks [113]. Ying et al. [49] utilized an aqueous phase containing two immiscible components—a cell/GelMA mixture and poly(ethylene oxide) (PEO)—as a bioink to fabricate pre-designed, cell-loaded hydrogel structures via photocrosslinking. They employed extrusion or stereolithography bioprinting with digital micromirror devices. The PEO phase was subsequently removed from the photocrosslinked GelMA hydrogels, resulting in microporous 3D-bioprinted structures. Their results demonstrated that cells encapsulated within these porous hydrogel structures exhibited higher viability, spreading, and proliferation compared to those in standard nonporous hydrogels (Fig. 4b). Messaoud et al. [114] developed an adjustable aqueous two-phase system composed of photocrosslinked GelMA and dextran. By varying the pH and dextran concentration, they generated microgels with three distinct architectures: homogeneous nonporous, regularly disconnected pores, and bicontinuous structures with interconnected pores. Their findings revealed that all three hydrogel types supported cell growth with distinct phenotypic characteristics, maintaining high viability and expected morphology after seven days of culture.

However, aqueous two-phase emulsified bioinks in this method exhibited instability and short storage time of only a few minutes before phase separation occurred, reducing their micro-reforming capacity. This limitation was particularly problematic in DLP-based bioprinting, where the bioink needed to remain in the liquid phase throughout the process; unexpected phase separation could compromise printing

Table 1 Emulsion method

Combination method		Printing method	Application	Advantage	Disadvantage
w/o	w/mineral oil [48] w/soybean oil [96] w/corn oil [97] w/peanut oil [98]	● Extrusion-based 3D bioprinting [48]	● Bone and cartilage tissue engineering [48]	● Easier to regulate the stability of the scaffold [108] ● Good cytocompatibility and allowing for the simultaneous embedding of cells [109]	● The incorporation of organic phases or surfactants is often biotoxic [48] ● The emulsion bioink is not stable [48]
w/w	GelMA/PEO [49] GelMA/dextran/GGMMA [99] GelMA/dextran [100] GelMA/PCL/PEO [101] SF-dECM/PEG [102]	● Extrusion-based 3D bioprinting [102, 104] ● DLP [100, 105] ● Pre-shear bioprinting [106]	● Wound healing [107] ● Bone and cartilage tissue engineering [100, 102] ● Lung cancer cell culture in vitro [105]	● The emulsion does not require biotoxic organic solvents [110] ● Higher cell viability, spreading, and proliferation [49]	● The microporous network is insufficient to meet the nutrient demands of large tissue structures [49] ● The limited time window for bioprinting [100]
Macromolecular crowding	$NaHCO_3$/PVP [103]	● DOD bioprinting [103]	● Reconstruction of the hierarchical porous structure [103] ● Fabrication of complex 3D tissue models [103]	● Accelerates the process of collagen fiber formation [103] ● Modulates the collagen structure in a controlled manner [103]	● Relatively little research and application [103]

GelMA: gelatin methacryloyl; PEO: poly(ethylene oxide); GGMMA: methacrylate galactoglucomannan; PCL: polycaprolactone; SF-dECM: silk fibroin and decellularized extracellular matrix; PEG: polyethylene glycol; DLP: digital light processing; PVP: polyvinylpyrrolidone; DOD: drop-on-demand

quality [100] (Table 1). To address this, Qin et al. [104] developed biosurfactant-stabilized rhamnolipid micropore-forming GelMA-based inks, while Tao et al. [108] formulated emulsion-based bioinks by mixing aqueous dextran microdroplets with GelMA solution, further stabilizing them with β-lactoglobulin nanoparticles. Their results demonstrated that incorporating biosurfactants significantly improved the stability of micropore-forming GelMA ink. To further enhance aqueous emulsion stability, Wang et al. [99] integrated the preparation and assembly of GelMA microgels into a ternary aqueous emulsion system. They incorporated plant-derived methacrylated galactoglucomannan (GGMMA) into a dispersed phase of GelMA droplets, using dextran as the continuous phase. Dextran removal through medium leaching facilitated micropore formation within the hydrogel structure, which in turn promoted cell proliferation and infiltration. Despite these advancements, generalizing this approach to other hydrogels remained challenging due to the requirement for phase separation in aqueous solutions. Additionally, microporous networks with pores up to tens of micrometers might be insufficient to meet the nutritional needs of larger tissue structures. The emulsion method also exhibited limited pore interconnectivity and bioink emulsion instability, restricting the viable time window for bioprinting.

Macromolecular crowding (MMC) occurs in both intercellular and intracellular spaces, influencing cellular biochemistry by regulating key processes such as protein folding and nucleic acid interactions. The core of this method was the emulsion process (Table 1). Ng et al. [103] proposed a single-step drop-on-demand (DOD) bioprinting strategy using a macromolecule-based bioink to fabricate hierarchically porous collagen-based hydrogels. They employed polyvinylpyrrolidone (PVP) as a printable polymer bioink and deposited nanometer-sized collagen monomers as droplets. Crosslinking agents ($NaHCO_3$) and PVP macromolecules were strategically positioned to control pore size within each printed collagen layer, enabling the formation of complex 3D hierarchically porous collagen structures. Experimental results demonstrated that in their bioprinting–macromolecular crowding process, the collagen structure (pore size and porosity) in each printed layer could be controlled by adjusting the PVP concentration. The presence of PVP macromolecules accelerated collagen fiber formation and modulated collagen structure in a controlled manner. These findings suggested that regulating the number of macromolecule-based bioink droplets printed on each collagen layer allowed for the fabrication of hierarchically porous collagen structures.

Advancements in the emulsion method have led to the development of various bioinks for wound dressing and healing. GelMA-based aqueous two-phase emulsion bioinks have been integrated into handheld bioprinting systems, allowing convenient, shape-controlled in situ bioprinting. The pore-forming properties of emulsion bioinks facilitated fluid and oxygen transport, as well as cell proliferation and spreading,

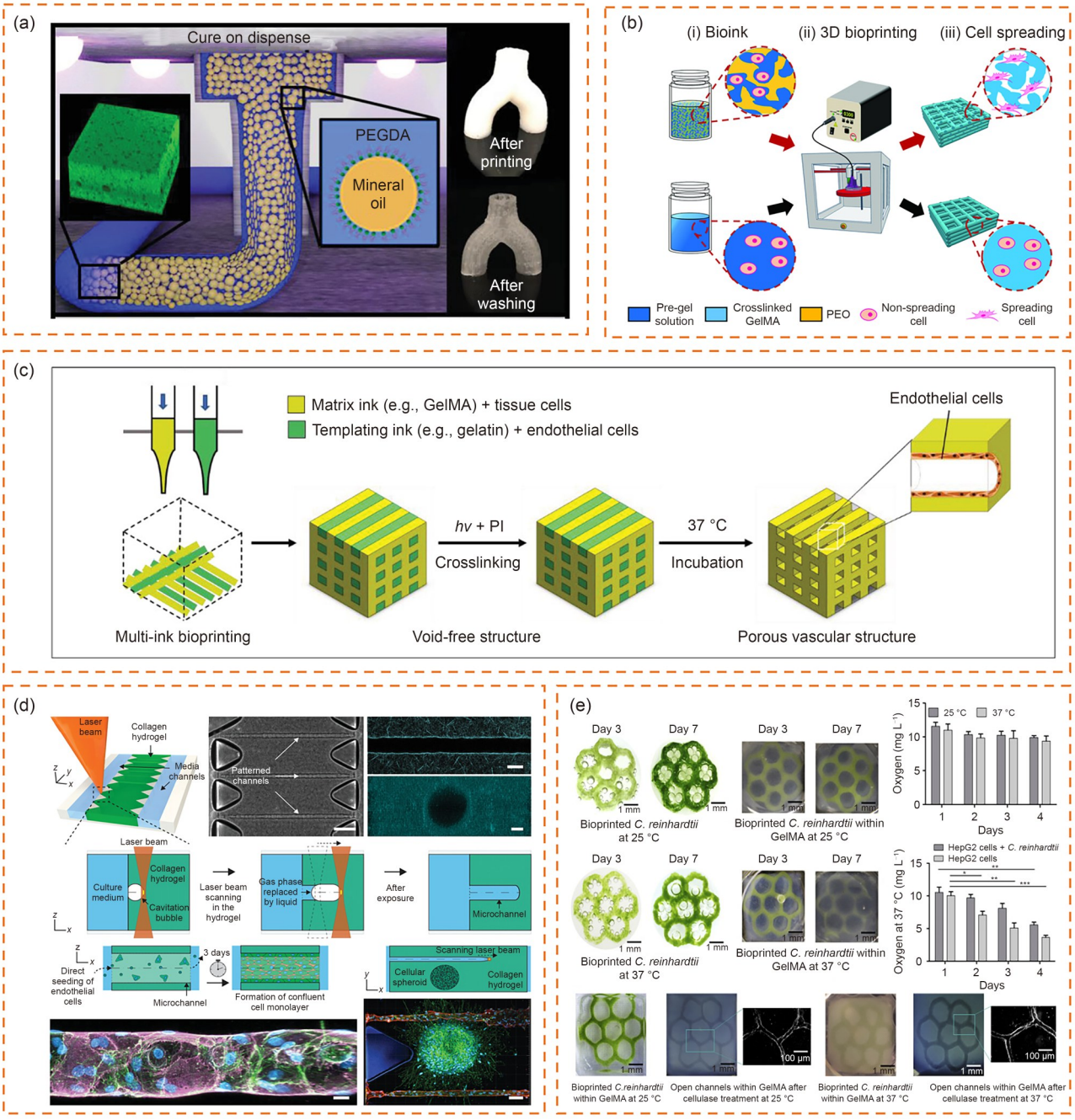

Fig. 4 Postprint processing. (a) Schematic representation of 3D printing hydrocolloid inks using cure-on-dispense to generate hierarchically porous structures. Reproduced from [111], Copyright 2018, with permission from WILEY-VCH Verlag GmbH & Co. KGaA, Weinheim. (b) Diagram illustrating the 3D bioprinting of a porous hydrogel structure using two-phase aqueous emulsion bioink, compared to a conventional hydrogel structure. Reproduced from [49], Copyright 2018, with permission from WILEY-VCH Verlag GmbH & Co. KGaA, Weinheim. (c) Schematic of the void-free 3D printing process, where a biocompatible templating bioink (green) and a matrix bioink (yellow) were printed side by side, followed by photocrosslinking of the matrix phase and incubation at 37 °C to release the templating phase. Reproduced from [50], Copyright 2019, with permission from the authors, licensed under CC BY. (d) 3D laser-based cavitation molding for vascularized tissue models. Reproduced from [129], Copyright 2022, with permission from the authors, licensed under CC-BY-NC-ND. (e) Growth of bioprinted *C. reinhardtii* and measurement of dissolved O_2 levels in the medium. Reproduced from [133], Copyright 2020, with permission from Elsevier Inc.

while maintaining flexibility to withstand repeated mechanical compression [107]. The combination of emulsion-based 3D bioprinting with stem cells holds significant potential for cranial defect reconstruction. Tao et al. [100] used GelMA and dextran biphasic emulsions to create porous scaffolds via DLP printing. Their results demonstrated that these scaffolds promoted cell proliferation, spreading, and bone defect repair. Zhang et al. [102] developed a bioink

composed of two immiscible aqueous phases, GelMA and dextran, to construct cartilage tissue structures. This approach enabled the formation of a crosslinker-free biological linkage with mechanical strength and biological activity comparable to the native cartilage extracellular matrix (ECM). Gonzalez-Fernandez et al. [115] introduced a non-viral, gene-activated bioink capable of controlling plasmid gene delivery to stem cells in both time and space. Their findings underscored the potential of emulsion-based methods for therapeutic gene delivery, enabling spatially directed stem cell differentiation and the engineering of complex tissues.

2.3.2 Expendable material method

The expendable material method is a direct 3D bioprinting strategy that enables the fabrication of complex, free-form 3D structures using tunable sacrificial bioinks. Under specific conditions, the sacrificial template is removed, creating an extensive pore network.

Various sacrificial inks have been explored (Table 2). Gelatin microgel, with its reversible thermal crosslinking mechanism and superior biological properties, has been widely used as a sacrificial ink [120]. Shao et al. [121] developed a sacrificial microgel bioink strategy featuring mesoscale pore networks (MPNs) for direct bioprinting, aiming to enhance nutrient delivery and cell growth. Their bioink, composed of a cell/GelMA mixture and gelatinized gelatin microgel, was first thermally crosslinked to fabricate predesigned, cell-loaded structures on a cold platform via extrusion bioprinting. The structure was then permanently stabilized through photocrosslinking with GelMA. The MPNs within the printed structure formed after the dissolution of the gelatin microgel. The results demonstrated that osteoblasts and human umbilical vein endothelial cells encapsulated in bioprinted, large-sized (⩾1 cm) MPNs exhibited enhanced bioactivity during culture. This finding suggests that their 3D bioprinting strategy improved cell survival in MPN-containing bioprinted structures and promoted the corresponding in vivo behavior of the encapsulated cells. Additionally, PEG, polyvinyl alcohol (PVA), and sugar particles have been used as sacrificial templates. Xu et al. [119] introduced a novel technique employing live bacteria as sacrificial porogens to create microporous hydrogel scaffolds. They mixed *Escherichia coli* with an agarose solution and solidified the mixture in a 12-well plate. The bacteria formed colonies within the hydrogel, which were later lysed. Subsequent washing with Dulbecco's phosphate-buffered saline and deionized (DI) water removed bacterial fragments and DNA, leaving behind a porous structure. This method enabled precise control over porosity, pore connectivity, and mechanical properties, facilitating dynamic scaffold design.

The expendable material method enabled the creation of complex porous structures with lower energy consumption, allowing modulation of the total void ratio while maintaining rheological properties suitable for bioprinting. This resulted in structures that promoted cell migration and infiltration [122]. During 3D printing, the presence of pores often led to structural instability, causing the top layer to buckle and deform the pores in the bottom layer [123]. Traditional

Table 2 Expendable material method

Expendable material	Base material	Sacrifice method	Application	Ref.
Pluronic F127	Alginate	● Washing	● Bone and cartilage tissue engineering	[116]
Gelatin microgel	GelMA	● Changing temperature	● Enhancement of cellular activities by facilitating the effective oxygen and nutrient diffusion	[117]
Gelatin templated microgel (gelatin/Pluronic F127/gum Arabic)	F-GelMA HAMA CSMA DexMA	● Changing temperature	● Enhancement of cellular activities ● Mineral formation in osteoblast-like cells	[117]
Dextran	PEGA GelMA SilMA	● Washing	● Enhancement of cellular activities ● Cartilage tissue engineering	[108]
PEO	GelMA	● Washing	● Enhancement of cellular activities	[49]
PVA	Alginate Agarose PRP	● Washing	● Enhancement of cellular activities ● Biomanufacturing of clinically relevant prevascularized tissues or organs	[118]
E. coli	Agarose	● Washing	● Permission to seed stem cells and other cell types	[119]

PEO: poly(ethylene oxide); GelMA: gelatin methacryloyl; F-GelMA: cold fish GelMA; HAMA: methacrylate hyaluronic acid; CSMA: methacrylate chondroitin sulfate; DexMA: methacrylate dextran; PEGA: 8-arm polyethylene glycol acrylate; SilMA: silk fibroin methacrylate; PVA: polyvinyl alcohol; PRP: platelet-rich plasma

expendable material methods sacrificed key advantages such as speed, simplicity, and the ability to additively manufacture matrix components. Additionally, post-seeding proved inefficient and poorly controlled, often leading to uneven cell distribution (Table 2). Ouyang et al. [50] developed a novel bioprinting method that fabricated complex 3D vascular networks in a single step, eliminating the need for material casting or late cell seeding. The researchers used two bioinks: a gelatin-based template and a photocrosslinkable matrix, printed side by side to form seamless 3D structures. After photocrosslinking, the gelatin liquefied at 37 °C, creating template channels. This approach prevented lattice bending, channel fusion, and swelling while enabling the formation of interconnected tubular pores and allowing the use of low-concentration bioinks. Compared to other sacrificial bioprinting strategies, it offered greater efficiency, uniformity, and control over cell density [50] (Fig. 4c). However, sacrificial templates exhibited limited in vivo remodeling capabilities due to their resistance to degradation by human cells. Additionally, maintaining different phases of gelatin porins during in vivo injections proved challenging due to variations in melting points. Hidalgo et al. [124] developed a porous injection system using photocrosslinked salmon gelatin and physically crosslinked porcine gelatin. In this system, porcine gelatin remained solid, while salmon gelatin remained liquid during injection. After injection and photocrosslinking, the porins degraded at physiological temperatures, forming a uniform porous structure. This method provided controlled gel kinetics, low viscosity, reduced injection force requirements, robust mechanical properties, and excellent cell compatibility.

Advances in the expendable material method have demonstrated significant potential for constructing tissue structures, regenerative medicine, organ printing, and drug delivery applications (Table 2). Zhou et al. [125] developed a catechol-functionalized ink system to fabricate scaffolds with enhanced toughness and elasticity, utilizing sacrificial gelatin to generate microchannels. Their findings indicated that the 3D printing platform, based on the sacrificial method, provided a promising approach for skin regeneration and could be further refined by incorporating additional cell types to construct functional skin tissues. Xie et al. [126] proposed an innovative bioink in which thermally crosslinked sacrificial gelatin microspheres, encapsulating human umbilical vein endothelial cells, were prepared using an electrospraying method as an auxiliary component. The GelMA precursor solution, mixed with the subject cells, served as the primary component. Their successful in vitro printing of human breast tumor tissues with angiogenesis validated the sacrificial method's capability to construct large, vascularized tissues at the centimeter scale. Shen et al. [127] utilized two types of bioinks for bone printing: one served as a matrix bioink, consisting of a photocrosslinked extracellular matrix hydrogel. Their work further demonstrated the expendable material method's potential for tissue repair.

2.3.3 Other methods (femtosecond laser/microalgae/recrystallization)

3D tissue models that replicate human physiology are essential for biomedical research and hold significant potential as tools for drug development. Integrating and defining the microvascular system within these models is critical for optimizing cellular function. However, conventional bioprinting methods primarily allow for the fabrication of hydrogel scaffolds containing vessel-like structures with large diameters and simple geometries [128]. Recent advances in laser photoablation have improved the resolution and complexity of these structures. However, the thermal ablation properties of this process, along with material decomposition, pose compatibility issues with protein hydrogels and embedded cells. To overcome these limitations, Enrico et al. [129] introduced a femtosecond laser-based method. In this approach, laser irradiation of the hydrogel generated cavitation bubbles, which rearranged collagen fibers to form stable microchannels. The use of femtosecond infrared laser pulses minimized thermal effects and mechanical stress, preserving cell viability while enabling the formation of 3D channels in hydrogels loaded with cells and organoids. Endothelial cell culture and cellular media perfusion further supported the creation of artificial microvessels. This method demonstrated strong potential for constructing 3D tissue models with complex microvascular structures, facilitating research on intricate tissue systems, including tumors and neural tissues (Fig. 4d).

Adequate and homogeneous oxygen (O_2) distribution is essential for cell growth, while insufficient oxygen supply has been shown to induce cell death in 3D tissue structures [130]. Due to the limited diffusion of oxygen in thick 3D matrices, hypoxia typically occurs, especially in the central regions, when the tissue structure exceeds a few hundred micrometers to several millimeters in thickness [131]. The microalgae method utilizes photosynthetic microalgae as an oxygen source within engineered tissue structures, particularly for porous scaffold formation. Lode et al. [132] employed 3D mapping techniques to embed *Chlamydomonas reinhardtii* (*C. reinhardtii*) into a 3D alginate scaffold. Under illumination, cell proliferation increased, and oxygen production rose rapidly during further incubation. They also developed a co-culture system that spatially organized human cells and microalgae within the scaffold, allowing microalgae to deliver oxygen or secondary metabolites as therapeutic agents. Maharjan et al. [133] incorporated bioprinted *C. reinhardtii* within sacrificial structures into GelMA-based hydrogel constructs containing liver-derived cells. They evaluated oxygen availability generated by *C. reinhardtii* and its ability to support

the viability and function of human liver-derived cells within the tissue constructs. Their findings demonstrated that the presence of bioprinted *C. reinhardtii* enhanced mammalian cell viability and function while reducing hypoxic conditions. Additionally, the endothelialization of hollow, perfusable microchannels—formed after the removal of the bioprinted *C. reinhardtii*-laden patterns—resulted in biologically relevant, vascularized mammalian tissue structures (Fig. 4e).

The microstructure of 3D scaffolds plays a critical role in determining their performance and applications. Both macropores (hundreds of microns in size) and micropores (a few microns in size) significantly influence cellular behaviors such as adhesion, migration, and proliferation within scaffolds [134]. However, precisely generating micropores in the few-micron range remains challenging with current methods. The recrystallization method presents a potential solution by combining 3D printing with immersion of recrystallized salts, allowing for the fabrication of scaffolds with controlled macropores and micropores. In this approach, a $CaCl_2$ solution was applied to the printed scaffold until it was fully covered. As the alginate scaffold dehydrated, NaCl crystals gradually formed within the matrix. Upon incubation in water, the dissolution of NaCl crystals generated numerous micropores within the alginate structure. The size and distribution of these micropores were controlled by adjusting the sodium ion concentration in the alginate ink. These micropores were tailored to enhance adsorption, protein delivery, and mechanical strength of the scaffold [135].

2.4 Comparison of fabrication methods

The efficiency of pore formation is a critical factor in microporous 3D bioprinting and varies based on whether the process belongs to preprint, inprint, or postprint. Preprint methods, such as the microsphere and microgel approaches, require the prior preparation of porous microspheres or microgels, which can reduce overall printing efficiency. In contrast, inprint methods facilitate natural pore formation during printing, eliminating the need for additional steps and improving pore-making efficiency. Postprint methods require extra processing to induce pores after printing, leading to lower efficiency [47].

The scalability of pore-making methods is critical for the success of microporous 3D bioprinting. Microgels, emerging as promising biomaterials, possess unique properties but have limitations such as poor scalability, reliance on additives like oils, and restriction to low-viscosity polymer solutions [67]. However, they offer greater structural integrity than liquid bioinks, making them suitable for specific applications [68]. In contrast, cryobioprinting enables highly controllable and reproducible micro- and macrostructures while producing scaffolds with excellent flexibility and water absorption, making it highly scalable [46]. Similarly, the microphase separation method allows for independent control of viscoelasticity, stiffness, and porosity, further enhancing scalability [47].

Different microporous 3D bioprinting methods offer distinct advantages for specific applications. Porous microsphere printing provides superior stacking ability, making it ideal for bone [52] and cartilage repair [136]. The microgel method, with its lower inherent flow behavior, is well-suited for cartilage repair [44] and wound healing [68]. Foam bioinks offer high flexibility, ductility, shape fidelity, structural stability, and strong adhesion to surrounding tissues, making them suitable for muscle fabrication [45]. Cryobioprinting enables the fabrication of controlled, anisotropic, interconnected microchannels, making it optimal for muscle-tendon repair [46]. Triggered micropore formation allows for the rapid fabrication of uniformly layered, cell-loaded hydrogels, making it effective for vocal cord repair [47]. The emulsion method, which provides greater control over scaffold stability, is used in bone [100] and cartilage repair [102]. The expendable material method enables modulation of the total void ratio while maintaining rheological properties suitable for bioprinting, making it applicable for neurofibril [137] and heart tissue fabrication [118].

3 Application

Conventional scaffolds often exhibit submicron or nanoscale structures or, in some cases, lack porosity, which restricts cell growth and proliferation [138]. Ideal microporous 3D scaffolds should mimic the ECM, creating an optimal microenvironment for cell migration and proliferation, thereby promoting tissue regeneration. In microporous 3D bioprinting, scaffolds fabricated using various techniques—such as those described above—are typically composed of biodegradable natural or synthetic biomaterials, cells, and bioactive factors. These scaffolds effectively control and guide localized tissue regeneration [139]. As a result, microporous 3D bioprinting shows significant promise for a wide range of applications, including the creation of artificial tissues and organs, as well as tissue defect repair.

3.1 Construction of artificial tissues and organs

3.1.1 Vasculature

Cells embedded within tissue structures require an optimal supply of nutrients and oxygen, as well as efficient waste removal, to remain viable and functional [140]. The diffusion of growth factors and other signaling biomolecules is equally essential for regulating cellular behavior. Large tissues and organs rely on a complex vascular system to ensure adequate

blood flow, deliver necessary nutrients, and sustain essential functions. Thus, incorporating vascular-like structures is crucial for constructing functional tissues suitable for regeneration and developing in vitro models for studying disease mechanisms and screening drug compounds [141].

To date, researchers have employed various biofabrication strategies and techniques to enhance the physiological relevance of vascular models and address the limitations of two-dimensional cell cultures. 3D bioprinting has been used to replicate complex blood vessel geometries. Techniques such as scaffold-free direct ink writing, embedded bioprinting, photo-assisted bioprinting, sacrificial molding, and coaxial bioprinting have all been applied to mimic the intricate structure of vascular networks [142]. Despite significant advancements in bioprinting technology, fabricating complex vascular structures remains challenging, as it requires printing bioinks that must simultaneously support living cells and maintain vascular integrity. These challenges have led some studies to explore alternatives beyond direct 3D printing for vascular structure fabrication. Shao et al. [106] proposed a pre-sheared bioprinting strategy to create highly oriented porous hydrogel microfibers for vascular tissue construction. They mixed a polymer thickener (PEO) with a hydrogel precursor (GelMA) to generate a viscous, porous bioink. When the GelMA/PEO solution passed through a transparent glass tube connected to a coaxial nozzle, the GelMA was photocrosslinked in situ, forming highly oriented porous microfibers. Additionally, they demonstrated the fabrication of heterogeneously oriented microfibers and their artificial assembly. When endothelial cell fibers and cancer cell fibers were cocultured and assembled, the cells exhibited growth behaviors similar to those observed in vivo.

Sacrificial bioprinting is widely used to construct vascularized tissues, typically by selectively removing fibers to create permeable channels. There are two main types of sacrificial templates: gelatin-based and carbohydrate-based [143]. Gelatin is commonly utilized due to its excellent biocompatibility, allowing endothelial cells to be directly encapsulated in gelatin bioinks during bioprinting. The gelatin solution solidifies at lower temperatures but liquefies at approximately 37 °C, facilitating the removal of gelatin-based sacrificial templates. Additionally, the strong mechanical properties of carbohydrates support the fabrication of multilayered, interconnected vascular systems on a larger scale [144]. Ouyang et al. [50] addressed two major challenges in tissue vascularization: maintaining structural fidelity and achieving effective endothelialization. They developed a versatile 3D bioprinting strategy that involved depositing template bioinks layer by layer alongside matrix bioinks to construct void-free, multimaterial structures. After the matrix phase was crosslinked, the template phase was sacrificed, creating a 3D network of interconnected tubular channels (Fig. 5a). The results demonstrated that this void-free 3D printing (VF-3DP) method efficiently cellularized the inner surface of the channels by preloading endothelial cells into the template bioink, forming a fused endothelial layer. This in situ endothelialization approach generated a more homogeneous endothelial cell distribution than the traditional post-seeding method. Currently, the sacrificial method remains the most common and effective approach for vascular construction.

3.1.2 Bone

Natural bone exhibits a hierarchical structure with pores spanning multiple length scales, and studies have shown that multiscale porosity enhances the in vitro and in vivo performance of scaffolds [145]. Pores of different sizes serve distinct functions: smaller, well-connected cell-scale pores promote cell proliferation, migration, and nutrient diffusion, while pores of at least 50 μm (ideally 300 μm) facilitate bone tissue deposition [146]. However, multiscale porosity is often overlooked in bone tissue scaffold fabrication, with pore sizes typically limited to a single order of magnitude. This constraint restricts cellular penetration into the bulk material, reducing mass transport and nutrient availability. To address this challenge, incorporating an additional layer of larger pores (>200 μm) into the scaffold can create an optimal multiscale pore structure for bone tissue, integrating three pore size categories: interconnections, standard pores, and large pores [147]. Moreover, the ECM of bone tissue forms a complex, multi-component microenvironment. Despite advances in fabrication techniques and synthetic materials, replicating its specificity and structural complexity remains a significant challenge.

Previous methods for generating larger pores in scaffolds focused on creating large water droplets in the initial emulsion. This was achieved by applying high temperatures or solvents to destabilize the emulsion in a controlled manner, allowing droplets to aggregate into larger ones. However, these methods altered the overall scaffold pore network, forming larger droplets rather than increasing overall porosity. Additionally, these approaches impacted pore connectivity. When the phase membrane surrounding neighboring droplets was sufficiently thin, pore interconnections formed during polymerization, leading to the development of small interconnected pores [148]. To overcome these limitations, Wang et al. [149] developed a bioprinting system based on combinable gradient DLP, integrating a microfluidic mixer to generate continuous or discrete gradients of the desired bioink in real time. Various planar and 3D structures exhibited continuous gradients in material composition, cell density, growth factor concentration, hydrogel stiffness, and porosity in both horizontal and vertical directions (Fig. 5b). To more accurately replicate the complex heterogeneous tissue patterns of natural bone, dual or multiple gradients in tissue-simulating structures are essential. Wang et al. [149]

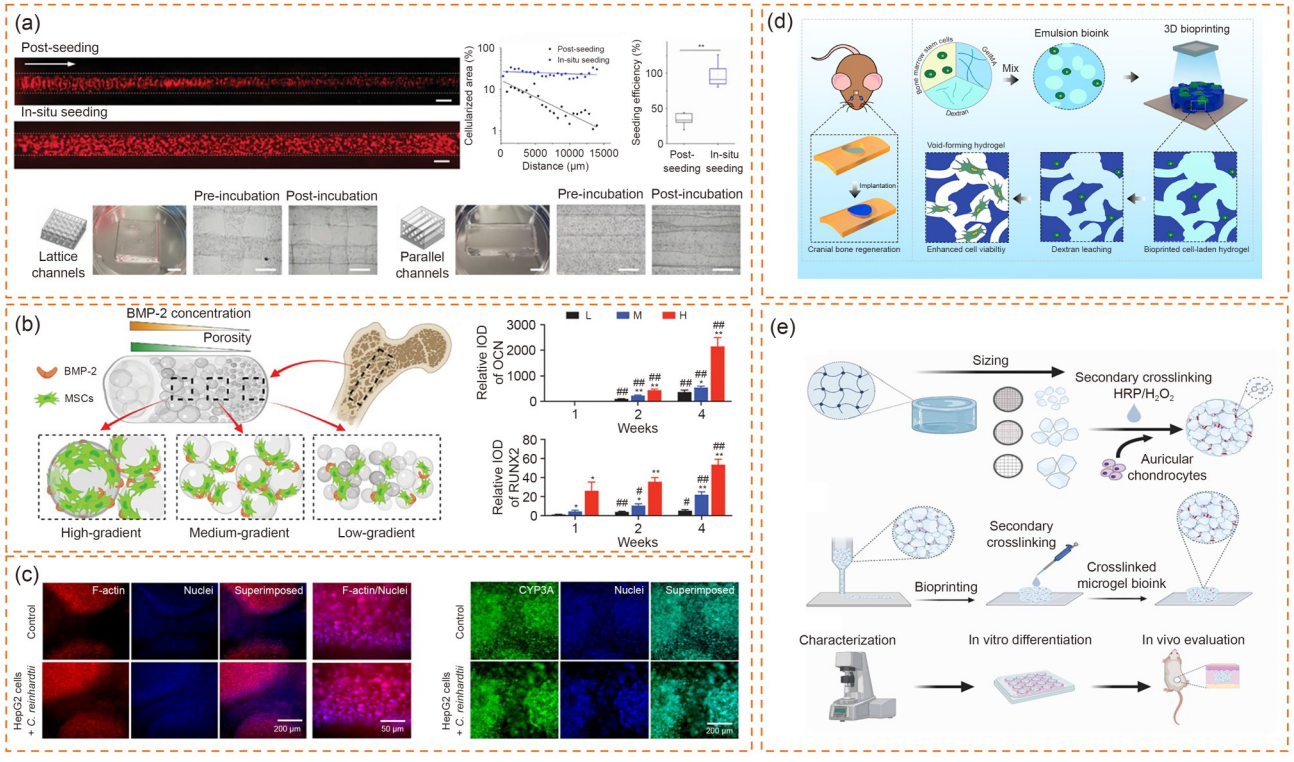

Fig. 5 Application of microporous 3D bioprinting. (a) Representative fluorescence micrographs comparing the conventional post-seeding method with in situ seeding, used to evaluate the homogeneity and efficiency of cell seeding. Reproduced from [50], Copyright 2019, with permission from the authors, licensed under CC BY. (b) Schematic of a bioprinted 3D construct encapsulated with MSCs, used to investigate the osteogenic effects of dual gradients of porosity and BMP-2. Reproduced from [149], Copyright 2021, with permission from Wiley-VCH GmbH. (c) Fluorescence micrographs showing the expression of F-actin (red) and CYP3A (green) by HepG2 cells within a GelMA construct at Day 7, with and without *C. reinhardtii*. Nuclei were counterstained with DAPI (blue). Reproduced from [133], Copyright 2020, with permission from Elsevier Inc. (d) Schematic illustration of 3D-bioprinted void-forming hydrogel constructs designed for implantation. Reproduced from [100], Copyright 2022, with permission from the authors, licensed under CC-BY-NC-ND. (e) Schematic of HA-TYR microgel bioinks with tunable porosity and their application in bioprinting cartilage tissues. Reproduced from [44], Copyright 2022, with permission from the authors, licensed under CC BY. DAPI: 4',6-diamidino-2-phenylindole

further incorporated a second biological gradient of bone morphogenetic protein 2 (BMP-2) into the porosity gradient structure to enhance osteogenesis in mesenchymal stem cells (MSCs). In a four-week osteogenesis study, MSCs in 3D constructs bioprinted with a dual gradient of BMP-2 and porosity grew in clusters, populating the pore regions of the hydrogel. Cell spreading and proliferation increased in areas with higher porosity. Additionally, immunofluorescence staining, gene expression analysis, and calcium deposition data strongly suggest that the dual gradient of porosity and BMP-2 effectively stimulated osteogenesis in MSCs, closely mimicking the structure of natural bone tissue.

High internal phase emulsions (HIPEs) have recently been explored for bone tissue engineering. Sengokmen-Ozsoz et al. [150] combined emulsion templating with 3D printing to examine how varying concentrations of tartrazine, used as a photoabsorber, influenced the porous structure of inner-phase emulsions in acrylate-based polymerization media prepared via vat photopolymerization. They evaluated cell behavior on 3D-printed disk samples using MG-63 cells, assessing metabolic activity, adhesion, and morphology. The results demonstrated that HIPEs could serve as resin for 3D printing trabecular bone mimics, with potential applications in developing lab-on-a-chip models for healthy and diseased bone tissue. Du et al. [151] developed a novel approach for designing polymeric high internal phase emulsion (polyHIPE) scaffolds with microchannels and multiscale porosity using 3D-printed water-soluble PVA sacrificial molds. This method utilized fused deposition modeling to produce two sacrificial mold variants filled with HIPE, which were later dissolved to form polyHIPE scaffolds containing microchannels. In vitro evaluations demonstrated that microchannels significantly enhanced cell infiltration, proliferation, and osteogenic differentiation, underscoring their beneficial effects on cell behavior. These findings have promising applications in bone tissue engineering and regenerative medicine and are expected to facilitate the clinical translation of such biomaterial scaffolds. Currently, the emulsion method remains the most widely used and suitable approach for biomanufacturing bone tissue.

3.1.3 Liver

The liver possesses a remarkable regenerative capacity, even after significant damage. Its functional unit, the hepatic lobule, is a hexagonal structure approximately 1 mm in length and 2 mm in thickness. These lobules perform essential roles in exocrine and endocrine metabolism, as well as detoxification. Collectively, millions of lobules form the Couinaud segments that constitute the liver [152]. In recent years, various techniques have been employed to create biomimetic liver tissues, beginning with two-dimensional cultures of parenchymal cells, which have demonstrated successful differentiation [153]. However, these simple techniques fail to replicate the complex microenvironment necessary for cell–ECM interactions, thereby limiting cell survival.

Recently, microporous 3D bioprinting techniques have been employed to fabricate liver-like microstructures. One study proposed a method using liver spheroids instead of individual liver cells in bioprinting. This approach protected cells from shear stress during the printing process and promoted volumetric cell–cell interactions. Bioprinted liver spheroids embedded in GelMA hydrogel maintained long-term functionality for up to 30 d, stably secreting liver biomarkers such as albumin, ceruloplasmin, alpha-1 antitrypsin (A1AT), and transferrin. These findings demonstrated that the microsphere method could be broadly applied in 3D bioprinting of liver tissues [154]. Maharjan et al. [133] embedded bioprinted *C. reinhardtii* sacrificial structures into GelMA-based hydrogel constructs containing liver-derived cells. They assessed the oxygen availability produced by bioprinted *C. reinhardtii* and its ability to support the viability and function of human liver-derived (HepG2) cells within tissue constructs (Fig. 5c). They also investigated the feasibility of forming hollow microchannels through incubation and enzymatic removal of bioprinted *C. reinhardtii* patterns, followed by endothelial cell implantation to create vascularized liver tissue-like structures. Currently, the microsphere method remains the most suitable and widely used approach for biomanufacturing liver tissues.

3.2 Tissue defect repair

3.2.1 Wound healing

The skin is the body's largest and fastest-growing organ, serving as a critical barrier against external damage. However, it is highly susceptible to injury. Traumatic wounds, such as third-degree burns and total dermal defects, pose significant challenges due to the skin's limited regenerative capacity. Consequently, donor skin tissues or bioengineered human skin constructs (HSCs) are often required to support the regeneration process [155]. In recent years, 3D-bioprinted skin structures have gained considerable attention for clinical applications in skin repair and transplantation. Most prior research on skin bioprinting has focused on using keratinocytes (KCs) and fibroblasts (FBs) to fabricate 3D skin structures, which typically lack intrinsic pigmentation. Melanocytes (MCs), essential components of the epidermal melanin unit, play a crucial role in skin pigmentation and are vital for developing more accurate in vitro skin models. While some studies have integrated MCs into 3D-bioprinted skin to create pigmented models [156], achieving consistent and homogeneous pigmentation remains a significant challenge requiring further investigation.

Microporous 3D bioprinting technology enables the precise deposition of various living cells and biomaterials, facilitating the fabrication of biomimetic tissue structures. Ng et al. [157] employed a two-step DOD bioprinting strategy, initially fabricating hierarchical porous collagen-based structures, followed by the deposition of epidermal cells. This method successfully generated biomimetic hierarchical porous structures resembling natural skin tissue. The results demonstrated that 3D-bioprinted skin structures exhibited greater similarity to natural skin than hand-cast samples, particularly in developing a well-stratified epidermal layer and a continuous basement membrane protein layer.

Skin regeneration involving skin appendages remains a significant challenge due to donor skin shortages, poor long-term viability, and the absence of appendages in HSCs for regeneration [158]. Zhou et al. [159] developed a novel method to fabricate functional living skin (FLS) using biomimetic bioinks with excellent biocompatibility and tissue adhesion, integrated with DLP-based 3D printing technology. The FLS contained interconnected microchannels that facilitated cell migration, proliferation, and new tissue formation. In vivo studies demonstrated that the FLS not only provided immediate defense functions but also significantly promoted dermal regeneration, including the regeneration of skin appendages in large animals.

The emulsion method has also been investigated for skin damage repair. Ying et al. [107] developed an open-source, portable, and ergonomic handheld bioprinting system that incorporated a two-phase water-emulsified bioink formulation. This biocompatible formulation enabled the encapsulation of cells during the wound dressing process. Additionally, in situ photocrosslinking produced a hydrogel dressing with interconnected micropores, facilitating the rapid transport of fluids and oxygen. These micropores also enhanced the survival, proliferation, and spreading of embedded cells, accelerating wound healing. Wang et al. [109] introduced a new bioink composed of two immiscible aqueous phases—GelMA and dextran—for skin damage repair, which also exhibited antibacterial and anti-inflammatory properties. This bioink can be printed using resin polymerization, extrusion, and handheld bioprinting techniques. The results demonstrated that the microporous structure formed after

3D bioprinting promoted the spreading of encapsulated cells, confirming the excellent cytocompatibility of the bioink formulation. Additionally, the bioink's antimicrobial and immunomodulatory properties provided an effective strategy to combat bacterial infections and support immunomodulation, both critical for wound healing. Currently, the emulsion method remains the most suitable for promoting wound healing.

3.2.2 Bone repairing

Bone defects remain a significant challenge in regenerative medicine [160]. Although bone possesses self-renewal capabilities, this regenerative potential is often impaired in cases of critical-size defects. Despite advances in the field, conventional treatments fail to meet the growing clinical demand for effective bone grafts due to limited availability, the risk of pathogen transmission, and reduced healing potential [161]. Studies have shown that well-designed microenvironments can alleviate these issues to some extent and are crucial for promoting bone regeneration [162]. Consequently, there is an urgent need to develop functional, bioactive scaffolds that can modulate the interactions between implants and host tissue, thereby facilitating the regeneration of bone defects.

Bone marrow stem cells (BMSCs), found in the mesenchymal compartment of the bone marrow, have the ability to self-renew and differentiate into specialized cells, presenting a promising pathway for bone regeneration [163]. In recent decades, various 3D printing methods incorporating BMSCs have been investigated for treating bone defects. Implanted BMSCs contribute to bone tissue regeneration by differentiating into osteoblasts, recruiting other therapeutic cells, and creating a favorable microenvironment through the release of paracrine factors [164]. However, directly delivering cell suspensions to the fracture site often results in suboptimal outcomes due to low survival rates, short retention time, and functional limitations. Recently, there has been growing interest in using hydrogel constructs, such as alginate and GelMA, for repairing bone defects with stem cells [165]. GelMA, which is based on a gelatin backbone, not only promotes the adhesion and proliferation of BMSCs [166], but also enables tunable mechanical properties through photopolymerization [167]. Furthermore, the microenvironment created by GelMA hydrogels supports osteogenesis in encapsulated BMSCs. However, the structural stability of GelMA hydrogels, typically achieved through a high degree of crosslinking and dense polymer networks, can limit nutrient diffusion and hinder cell migration and proliferation [49].

3D bioprinting technologies have diverse applications in the fabrication of high-performance bone tissue structures [168]. These technologies allow for precise spatiotemporal regulation of cell–cell and cell–ECM interactions, leading to structurally complex and functionally relevant tissue constructs. Among these, extrusion-based bioprinting has been commonly employed to create bone tissue structures due to its accessibility, cost-effectiveness, simplicity, and ease of handling [169]. However, extrusion-based methods can compromise the integrity of bone tissue structures and reduce fabrication speed due to interfacial artifacts between print lines and the continuous writing process, limiting their clinical applicability. In contrast, DLP-based 3D bioprinting platforms have been shown to produce structures with superior speed, resolution, and structural integration [170]. Zhang et al. [171] developed a Haversian bone-mimetic structure using DLP-based printing technology to promote new bone and blood vessel formation, demonstrating the potential of advanced 3D printing techniques for building bone tissue structures. Tao et al. [100] developed a therapeutic cell-loaded hydrogel for bone regeneration, incorporating pores. This hydrogel, created using DLP-based bioprinting with BMSCs mixed with a GelMA/dextran emulsion (Fig. 5d), was designed to modulate the behavior and function of encapsulated BMSCs for bone tissue regeneration. Their results showed that the 3D-bioprinted hydrogel not only promoted the proliferation, migration, and spreading of encapsulated BMSCs but also activated the YAP signaling pathway, enhancing osteogenic differentiation. Furthermore, the study demonstrated the microporous structure's effectiveness in repairing a 6-mm cranial defect, promoting new bone formation and facilitating potential clinical applications. Currently, both emulsion and sacrificial methods are considered more suitable for repairing bone defects.

3.2.3 Cartilage repairing

Cartilage, a vital connective tissue found in joints, ears, and the nose, lacks blood vessels and nerves, making self-repair particularly challenging. Cartilage tissue engineering aims to address this limitation by creating cell-loaded implants. 3D bioprinting has excelled in this field due to its precise spatial control, enabling it to closely mimic the structure and composition of natural cartilage [172].

A significant challenge in 3D bioprinting of cartilage tissues is identifying biologic linkage formulations that offer both high biocompatibility and printability. Although GelMA hydrogels support chondrocyte encapsulation, their prepolymer solutions typically exhibit low viscosity, compromising the fidelity of printed structures. Schuurman et al. [173] reported the use of GelMA/hyaluronic acid (HA) composites as bioinks for cartilage bioprinting. Histological and immunohistochemical staining of cell-laden constructs after four weeks of in vitro culture confirmed glycosaminoglycan formation and cartilage matrix production. Similarly, Markstedt et al. [174] developed a composite bioink comprising cellulose nanofibers and alginate, which demonstrated shear-thinning properties

suitable for extrusion-based 3D bioprinting. Human chondrocytes were encapsulated within this bioink, enabling the fabrication of both simple mesh-like structures and complex 3D auricular models.

Microtia refers to a group of congenital malformations of the outer ear that arise from various etiological and multifactorial factors. Although allograft implants are sometimes used for treatment, these biomaterials have limited biocompatibility and pose risks such as infection, erosion, and displacement. Consequently, there remains a need for biocompatible, mechanically stable implants capable of accurately reconstructing the complex shape of the outer ear while promoting auricular cartilage regeneration [175]. Microgel-based biomaterials present a promising alternative to traditional hydrogels for 3D bioprinting applications. These microgels comprised solid particles that were tightly packed through processes such as annealing or centrifugation, forming microporous scaffolds. Granular hydrogels have been widely used in cartilage tissue engineering. For instance, Flégeau et al. [44] developed tyramine-modified hyaluronic acid (HA-TYR) hydrogels, which were enzymatically crosslinked using horseradish peroxidase and hydrogen peroxide (H_2O_2). These crosslinked gels were screened using metal grids with varying pore sizes. The residual tyramine fraction facilitated secondary crosslinking, further stabilizing the scaffolds (Fig. 5e). Bioprinting microgels loaded with human auricular chondrocytes resulted in the uniform development of cartilage-like tissue in vitro, with mechanical strength reaching up to 200 kPa after 63 d. Additionally, when implanted subcutaneously in nude mice, microgel scaffolds with a 40-μm grid structure exhibited excellent tissue maturation and stability. This study underscored the critical role of porosity in the in vivo maturation of 3D-printed scaffolds. Currently, the microgel method holds significant promise for cartilage defect repair.

The applications and the corresponding common pore-making methods are listed in Table 3, while the comparison of fabrication methods is summarized in Table 4.

3.3 Emerging methods and applications

Advancements in tissue engineering and regenerative medicine have established the beneficial effects of bioelectricity on excitable tissue regeneration, including enhanced cell proliferation, differentiation, migration, and overall tissue function. Conductive biomaterials have emerged as valuable tools for promoting excitable tissue regeneration by facilitating the delivery of endogenous bioelectricity or electrical stimulation to electrically isolated cells and tissues [193]. Porous biomaterials have been used to enhance electrical conductivity for long-term applications by incorporating conductive components into the pre-solution during material preparation or by depositing conductive materials onto the internal pore surfaces [194]. These porous conductive biomaterials offer several advantages, such as increased specific surface area, reduced density, improved deformability, rough surface topology, and enhanced permeability. The presence of pores extends conductive pathways and increases material thickness, which may result in relatively low conductivity and modulus [139]. Furthermore, the rough surfaces and micropores of conductive porous biomaterials have been shown to promote the adhesion and migration of excitable cells. Some of these materials have also supported 3D cell cultures by allowing cells to migrate into interconnected pores [195]. Wang et al. [196] employed near-field electrostatic printing and graphene oxide coatings to fabricate 3D conductive porous scaffolds based on printed microfiber structures. In this process, graphene oxide was applied to poly (L-lactic acid-co-caprolactone) microfibers via layer-by-layer assembly and then reduced in situ to form reduced graphene oxide, resulting in a conductive porous scaffold with 25–50 layers of graphene oxide. Under electrical stimulation, the scaffold exhibited excellent electrical conductivity and successfully induced the formation of neuron-like networks along the conductive microfibers. Given its ability to guide nerve cell growth, this conductive porous scaffold holds significant potential for applications in nerve regeneration and neural engineering.

Embedded 3D printing (EB3DP) is an emerging technology that enables free-form fabrication within a soft substrate to support patterned materials, allowing for increased complexity and control in printing sacrificial templates. A key challenge in EB3DP is the lack of a stable ink-support matrix combination that simultaneously offers a high degree of freedom, low processing barriers, and high error tolerance during

Table 3 Application and its common pore-making method

Application	1st method	2nd method	3rd method
Construct vasculature	The sacrificial method [50, 116, 124, 176, 177]	The emulsion method [48, 104, 106, 113]	The cryobioprinting [46]
Construct bone	The emulsion method [100, 101, 104, 115, 150]	The microsphere method [136, 178–181]	The sacrificial method [117, 124]
Construct liver	The microsphere method [133, 182–185]	The sacrificial method [59, 116, 117, 125]	Recrystallization method [135]
Wound healing	The emulsion method [49, 79, 107, 110]	The sacrificial method [117, 124, 186]	The microgel method [68]
Bone repairing	The emulsion method [100, 104, 110, 113]	The sacrificial method [116, 127]	The gas method [74]
Cartilage repairing	The microgel method [44, 67, 68, 71]	The emulsion method [101, 102]	The sacrificial method [187]

Table 4 Fabrication method

Method		Printing method	Application	Efficiency	Scalability	Application-specific suitability
Preprint processing	Porous microsphere printing	● Extrusion [52] ● DLP [188]	● Biomanufacturing vasculature [59] ● Biomanufacturing cartilage [136] ● Biomanufacturing bone [52] ● Biomanufacturing liver [189]	● Low [52]	● Medium [52]	● Low [52]
	Microgel method	● Extrusion [71] ● DLP [190]	● Cartilage repairing [44] ● Wound healing [68]	● Medium [44]	● Low [69, 70]	● Low [68]
	Gas method	● Extrusion [45, 75]	● Muscle repairing [45] ● Biomanufacturing bone [75] ● Biomanufacturing vasculature [74]	● Medium [45]	● Low [45]	● High [45]
Inprint processing	Cryobioprinting	● Vertical freeze printing [46]	● Biomanufacturing muscle [46] ● Wound healing [84]	● Medium [46]	● High [85]	● Low [46]
	Triggered micropore forming	● Microphase separation [47]	● Biomanufacturing the vocal fold [47] ● Cancer modeling in vitro [47]	● High [95]	● High [47]	● Medium [47]
Postprint processing	Emulsion method	● DLP [100] ● Extrusion [107] ● Macromolecular crowding [103] ● Pre-shear bioprinting [106]	● Wound healing [107] ● Bone regeneration [100] ● Biomanufacturing cartilage [102]	● Medium [108]	● Medium [48, 49]	● Medium [48]
	Expendable material method	● Extrusion [176] ● Coaxial printing [191] ● Photocrosslinking [127]	● Biomanufacturing vessel [191, 192] ● Bone repairing [127] ● Biomanufacturing muscle [176] ● Neurofibril fabrication [137] ● Biomanufacturing heart [118]	● Low [122]	● Medium [123]	● High [121]
	Others	● Femtosecond laser [129] ● Extrusion [133, 135]	● Biomanufacturing liver [133] ● Capillary fabrication [129]	● Medium [129, 133, 135]	● Medium [129]	● Medium [133]

DLP: digital light processing

printing [197]. To address this issue, Wang et al. [198] developed a simple yet effective sacrificial strategy for creating a network of layered, fusible microchannels within a multifunctional porous scaffold. This approach integrated EB3DP, tunable polyelectrolyte complex (PEC), and casting techniques. The results demonstrated the feasibility of generating hierarchical channel networks within scaffolds while providing a reliable method for rapidly and reproducibly forming arbitrary patterns with spatial organization, cell heterogeneity, and complexity for tissue engineering and other applications. Another challenge in the field is fabricating solid fibers with ultra-fine diameters or tubular fibers with ultra-thin walls. While significant progress has been made in bioprinting larger freestanding filamentary tissues, achieving these finer structures remains difficult [199]. To address this, Tang et al. [200] developed a bioprinting strategy for producing both solid and hollow fibers with tunable sizes across a broad range. This method employed an aqueous two-phase embedded bioprinting technique combined with a specialized crosslinking and extrusion process. As a result, a freestanding, alginate-free aqueous architecture was created, enabling the free-form patterning of aqueous bioinks.

As tissue engineering continues to advance, innovations in scaffold delivery remain equally critical. Minimally invasive injections of tissue-engineered scaffolds offer benefits such as smaller incisions and faster recovery. However, designing an injectable scaffold presents a significant challenge. Xie et al. [201] developed a novel shrunken scaffold that was freeze-dried to remove moisture and then placed in a humid environment. Exposure to humidity caused the dry scaffold to shrink by up to 90%, while it rapidly expanded back to its original size and shape after use. They also designed a tool for minimally invasive scaffold delivery and demonstrated its potential to overcome limitations in current technologies that hindered the clinical repair of soft tissue defects through minimally invasive injections. In a similar effort to enhance 3D printing capabilities in tissue engineering, Gong et al. [202] introduced a composite-induced resolution enhancement strategy called "shrinking printing." This method relied solely on postprint processing of hydrogel structures. By immersing a 3D-printed hydrogel pattern, composed of a network of hydrophilic polyionic polymers, into a polyionic solution with the opposite net charge, rapid shrinkage occurred, resulting in varying degrees of size reduction relative to the original pattern. This technique improved resolution through post-processing without requiring modifications to printer hardware or most ink compositions.

4 Conclusions

The limitations of early 3D bioprinting technology, particularly in controlling porosity and aligning pores, have hindered the fabrication of multiscale, multifunctional microporous networks in bioprinted tissues. Although increasing porosity can enhance the biological properties of bioprinted tissues, it often compromises mechanical integrity (Fig. 6a). As 3D bioprinting technology has advanced, growing evidence suggests that a material's physical properties significantly impact its performance in practical applications. For instance, harder basal planes promote osteogenic differentiation, whereas softer basal planes facilitate chondrogenic differentiation. This underscores the potential of 3D bioprinting for creating complex macro–micro structures and the necessity of considering how structural and mechanical properties influence cellular behavior in bioinks. Huebsch et al. [40] demonstrated that modifying the matrix modulus through the introduction of a pore-forming agent produced microporous materials that not only improved cell viability but also enhanced cell spreading. Their findings indicated that stress relaxation played a critical role in matrix deposition by chondrocytes, with faster relaxation leading to greater matrix deposition and morphology more closely resembling articular chondrocytes under physiological conditions. Thus, the strategic incorporation of microporosity helps balance

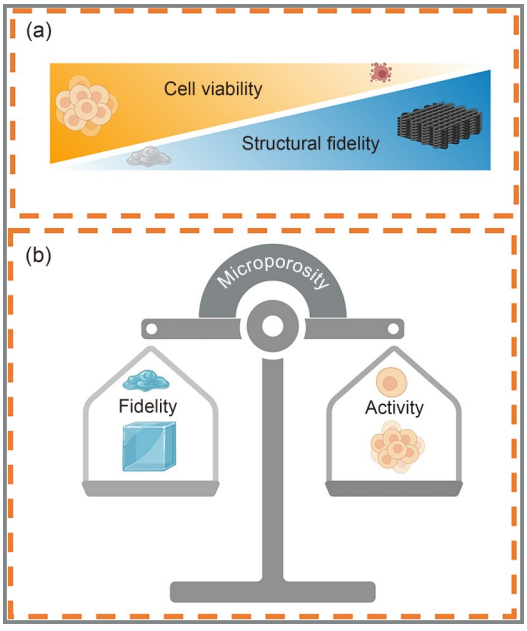

Fig. 6 Fidelity and activity. (a) Cell viability and structural fidelity exhibit an inverse relationship, where an increase in one often leads to a decrease in the other. (b) The role of microporosity in balancing structural fidelity and cellular activity

the physical and biological properties of bioprinted tissues, supporting cell survival, migration, osmosis, and material exchange within the body (Fig. 6b).

To replicate the structural heterogeneity and functionality of natural tissues and organs, researchers have explored various microporous 3D bioprinting methods, including preprint, inprint, and postprint processing, to regenerate functional tissue structures and repair defects. Microporous 3D bioprinting not only meets the mechanical requirements of bioprinted tissues but also provides essential biological properties, such as long-term cell survival, migration, osmosis, and material exchange. Despite these advancements, current microporous 3D bioprinting techniques still face challenges. For instance, extrusion-based methods, such as porous microsphere printing, lack the resolution and speed required for large-scale tissue fabrication. The emulsion method suffers from limited pore interconnectivity and instability in the bioink emulsion, reducing the available bioprinting time window. The expendable material method is hindered by low processing speed, complexity, and difficulties in additively manufacturing substrate parts. Additionally, bioprinted tissues produced with this approach often exhibit uneven cell distribution within the template channel, while sacrificial templates have limited remodeling capabilities in vivo. Future research should focus on developing new microporous 3D bioprinting techniques that enable efficient tissue printing optimized for human applications. These methods must support the normal growth, proliferation, migration, and homogeneous distribution of seed cells. Moreover,

addressing the challenge of microporous 3D bioprinting for large-scale tissue fabrication remains a critical priority.

Researchers recently developed a cell-adapted nanocolloid hydrogel for 3D printing mature tissue structures [203]. After implantation in the human body, these structures successfully matured into cartilage tissue, demonstrating potential for applications in articular cartilage defect repair and ear cartilage reconstruction. These findings highlight the promise of 3D bioprinting with cell-adapted nanocolloidal hydrogels for future clinical use. Innovations in bioprinting devices and technologies continue to expand the capabilities of porous bioprinting. Bioprinting devices are evolving from stationary desktop models to portable formats, with ongoing research focused on developing handheld and combination-carrying models. These advancements aim to integrate bioprinting into operating rooms and emergency frontline scenarios [204]. Meanwhile, improvements in printing technology have significantly influenced the field. Initially based on droplet inkjet printing, advancements in polymer types, crosslinking methods, and molding techniques have led to new approaches, such as acoustically triggered crosslinking. This method utilizes controlled acoustic fields to achieve high-resolution patterning. For example, researchers have explored self-enhancing ultrasound ink for deep-penetration acoustic volumetric printing and focused ultrasound writing techniques. These approaches offer key advantages, including low acoustic flow, rapid acoustic temperature polymerization, and increased print depth, enabling the fabrication of volumetric hydrogels and nanocomposites in diverse shapes, independent of optical properties [205]. Given the superior penetration of acoustic waves compared to light, bioprinting can be performed in vivo or within deeper tissues [206]. Future advancements in bioinks are essential to enhance the mechanical properties necessary for stabilizing bioprinted structures. For example, bioinks containing electrosprayed cell-loaded microgels combined with GelMA precursor solutions could improve these properties [207]. Additionally, integrating biological compounds to enhance cell interactions and create an optimal environment for generating physiologically relevant, vascularized tissues will be crucial for successful transplantation and integration with host tissues. As instrumentation technology, spatial and temporal resolution, bioink formulations, and microporous printing methods continue to advance, microporous 3D bioprinting is expected to become one of the most efficient, reliable, and advanced bioprinting technologies.

Acknowledgements This work was supported by the National Natural Science Foundation of China (Nos. 82302786 and 82172394), the China Postdoctoral Science Foundation (Nos. BX20230245 and 2023M742478), the Sichuan Science and Technology Program (No. 2023YFH0068), the Sichuan Province Innovative Talent Funding Project for Postdoctoral Fellows (No. BX202203), the Sichuan University Postdoctoral Interdisciplinary Innovation Fund (No. JCXK2226), 1·3·5 Project for Disciplines of Excellence, West China Hospital, Sichuan University (No. ZYGD23033), and the Postdoctoral Research Fund of West China Hospital, Sichuan University (No. 2023HXBH012).

Author contributions Writing—original draft: HXC and YRC; writing—review & editing: ZCD, JXF, YHL, CH, BYJ, and CZ; funding acquisition: ZKZ and ZYL; supervision: ZKZ, XCZ, and ZYL.

Declarations

Conflict of interest The authors declare that they have no conflict of interest.

Ethical approval This article does not contain any studies with human or animal subjects performed by any of the authors.

References

1. Vijayavenkataraman S, Yan WC, Lu WF et al (2018) 3D bioprinting of tissues and organs for regenerative medicine. Adv Drug Deliv Rev 132:296–332. https://doi.org/10.1016/j.addr.2018.07.004
2. Murphy SV, Atala A (2014) 3D bioprinting of tissues and organs. Nat Biotechnol 32(8):773–785. https://doi.org/10.1038/nbt.2958
3. Ravanbakhsh H, Karamzadeh V, Bao GY et al (2021) Emerging technologies in multi-material bioprinting. Adv Mater 33(49): 2104730. https://doi.org/10.1002/adma.202104730
4. Li XD, Liu BX, Pei B et al (2020) Inkjet bioprinting of biomaterials. Chem Rev 120(19):10793–10833. https://doi.org/10.1021/acs.chemrev.0c00008
5. Chen XB, Fazel Anvari-Yazdi A, Duan X et al (2023) Biomaterials/Bioinks and extrusion bioprinting. Bioact Mater 28:511–536. https://doi.org/10.1016/j.bioactmat.2023.06.006
6. Liang RJ, Gu YQ, Wu YC et al (2021) Lithography-based 3D bioprinting and bioinks for bone repair and regeneration. ACS Biomater Sci Eng 7(3):806–816. https://doi.org/10.1021/acsbiomaterials.9b01818
7. Jing SB, Lian LM, Hou YY et al (2024) Advances in volumetric bioprinting. Biofabrication 16(1):012004. https://doi.org/10.1088/1758-5090/ad0978
8. Jung O, Thomas A, Burks SR et al (2022) Neuroinflammation associated with ultrasound-mediated permeabilization of the blood–brain barrier. Trends Neurosci 45(6):459–470. https://doi.org/10.1016/j.tins.2022.03.003
9. Dababneh AB, Ozbolat IT (2014) Bioprinting technology: a current state-of-the-art review. J Manuf Sci Eng 136(6):061016. https://doi.org/10.1115/1.4028512
10. Christensen K, Xu CX, Chai WX et al (2015) Freeform inkjet printing of cellular structures with bifurcations. Biotechnol Bioeng 112(5):1047–1055. https://doi.org/10.1002/bit.25501
11. Kołodziejska M, Jankowska K, Klak M et al (2021) Chitosan as an underrated polymer in modern tissue engineering. Nanomaterials 11(11):3019. https://doi.org/10.3390/nano11113019
12. Muthukrishnan L (2021) Imminent antimicrobial bioink deploying cellulose, alginate, EPS and synthetic polymers for 3D bioprinting of tissue constructs. Carbohydr Polym 260:117774. https://doi.org/10.1016/j.carbpol.2021.117774

13. Yao ZM, Feng X, Wang ZL et al (2024) Techniques and applications in 3D bioprinting with chitosan bio-inks for drug delivery: a review. Int J Biol Macromol 278:134752. https://doi.org/10.1016/j.ijbiomac.2024.134752
14. Ferreira AM, Gentile P, Chiono V et al (2012) Collagen for bone tissue regeneration. Acta Biomater 8(9):3191–3200. https://doi.org/10.1016/j.actbio.2012.06.014
15. de Melo BAG, Jodat YA, Cruz EM et al (2020) Strategies to use fibrinogen as bioink for 3D bioprinting fibrin-based soft and hard tissues. Acta Biomater 117:60–76. https://doi.org/10.1016/j.actbio.2020.09.024
16. Łabowska MB, Cierluk K, Jankowska AM et al (2021) A review on the adaption of alginate-gelatin hydrogels for 3D cultures and bioprinting. Materials 14(4):858. https://doi.org/10.3390/ma14040858
17. Chen H, Xue H, Zeng H et al (2023) 3D printed scaffolds based on hyaluronic acid bioinks for tissue engineering: a review. Biomater Res 27(1):137. https://doi.org/10.1186/s40824-023-00460-0
18. Yue K, Trujillo-de Santiago G, Alvarez MM et al (2015) Synthesis, properties, and biomedical applications of gelatin methacryloyl (GelMA) hydrogels. Biomaterials 73:254–271. https://doi.org/10.1016/j.biomaterials.2015.08.045
19. Pescosolido L, Schuurman W, Malda J et al (2011) Hyaluronic acid and dextran-based semi-IPN hydrogels as biomaterials for bioprinting. Biomacromolecules 12(5):1831–1838. https://doi.org/10.1021/bm200178w
20. Purcell EK, Singh A, Kipke DR (2009) Alginate composition effects on a neural stem cell-seeded scaffold. Tissue Eng Part C Methods 15(4):541–550. https://doi.org/10.1089/ten.tec.2008.0302
21. Rajan N, Habermehl J, Coté MF et al (2006) Preparation of ready-to-use, storable and reconstituted type I collagen from rat tail tendon for tissue engineering applications. Nat Protoc 1(6): 2753–2758. https://doi.org/10.1038/nprot.2006.430
22. Jin HJ, Cho YH, Gu JM et al (2011) A multicellular spheroid formation and extraction chip using removable cell trapping barriers. Lab Chip 11(1):115–119. https://doi.org/10.1039/C0LC00134A
23. Schrobback K, Klein TJ, Crawford R et al (2012) Effects of oxygen and culture system on in vitro propagation and redifferentiation of osteoarthritic human articular chondrocytes. Cell Tissue Res 347(3):649–663. https://doi.org/10.1007/s00441-011-1193-7
24. Akkouch A, Yu Y, Ozbolat IT (2015) Microfabrication of scaffold-free tissue strands for three-dimensional tissue engineering. Biofabrication 7(3):031002. https://doi.org/10.1088/1758-5090/7/3/031002
25. Xu CX, Chai WX, Huang Y et al (2012) Scaffold-free inkjet printing of three-dimensional zigzag cellular tubes. Biotechnol Bioeng 109(12):3152–3160. https://doi.org/10.1002/bit.24591
26. Hospodiuk M, Dey M, Sosnoski D et al (2017) The bioink: a comprehensive review on bioprintable materials. Biotechnol Adv 35(2):217–239. https://doi.org/10.1016/j.biotechadv.2016.12.006
27. Nordberg RC, Bielajew BJ, Takahashi T et al (2024) Recent advancements in cartilage tissue engineering innovation and translation. Nat Rev Rheumatol 20(6):323–346. https://doi.org/10.1038/s41584-024-01118-4
28. Guillotin B, Guillemot F (2011) Cell patterning technologies for organotypic tissue fabrication. Trends Biotechnol 29(4):183–190. https://doi.org/10.1016/j.tibtech.2010.12.008
29. Wettergreen MA, Bucklen BS, Starly B et al (2005) Creation of a unit block library of architectures for use in assembled scaffold engineering. Comput Aided Des 37(11):1141–1149. https://doi.org/10.1016/j.cad.2005.02.005
30. Ferris CJ, Gilmore KJ, Beirne S et al (2013) Bio-ink for on-demand printing of living cells. Biomater Sci 1(2):224–230. https://doi.org/10.1039/C2BM00114D
31. Hölzl K, Lin SM, Tytgat L et al (2016) Bioink properties before, during and after 3D bioprinting. Biofabrication 8(3):032002. https://doi.org/10.1088/1758-5090/8/3/032002
32. Jayasinghe SN (2011) Bio-electrosprays: from bio-analytics to a generic tool for the health sciences. Analyst 136(5):878–890. https://doi.org/10.1039/C0AN00830C
33. Xu F, Celli J, Rizvi I et al (2011) A three-dimensional in vitro ovarian cancer coculture model using a high-throughput cell patterning platform. Biotechnol J 6(2):204–212. https://doi.org/10.1002/biot.201000340
34. Eiselt P, Yeh J, Latvala RK et al (2000) Porous carriers for biomedical applications based on alginate hydrogels. Biomaterials 21(19):1921–1927. https://doi.org/10.1016/S0142-9612(00)00033-8
35. Al-Munajjed AA, Hien M, Kujat R et al (2008) Influence of pore size on tensile strength, permeability and porosity of hyaluronan-collagen scaffolds. J Mater Sci Mater Med 19(8):2859–2864. https://doi.org/10.1007/s10856-008-3422-5
36. Douglas AM, Fragkopoulos AA, Gaines MK et al (2017) Dynamic assembly of ultrasoft colloidal networks enables cell invasion within restrictive fibrillar polymers. Proc Natl Acad Sci USA 114(5):885–890. https://doi.org/10.1073/pnas.1607350114
37. He Y, Yang FF, Zhao HM et al (2016) Research on the printability of hydrogels in 3D bioprinting. Sci Rep 6:29977. https://doi.org/10.1038/srep29977
38. Xin SJ, Wyman OM, Alge DL (2018) Assembly of PEG microgels into porous cell-instructive 3D scaffolds via thiol-ene click chemistry. Adv Healthc Mater 7(11):1800160. https://doi.org/10.1002/adhm.201800160
39. Zeltinger J, Sherwood JK, Graham DA et al (2001) Effect of pore size and void fraction on cellular adhesion, proliferation, and matrix deposition. Tissue Eng 7(5):557–572. https://doi.org/10.1089/107632701753213183
40. Huebsch N, Lippens E, Lee K et al (2015) Matrix elasticity of void-forming hydrogels controls transplanted-stem-cell-mediated bone formation. Nat Mater 14(12):1269–1277. https://doi.org/10.1038/nmat4407
41. Gupta D, Vashisth P, Bellare J (2021) Multiscale porosity in a 3D printed gellan–gelatin composite for bone tissue engineering. Biomed Mater 16(3):034103. https://doi.org/10.1088/1748-605x/abf1a7
42. Bible E, Chau DYS, Alexander MR et al (2009) Attachment of stem cells to scaffold particles for intra-cerebral transplantation. Nat Protoc 4(10):1440–1453. https://doi.org/10.1038/nprot.2009.156
43. Qutachi O, Vetsch JR, Gill D et al (2014) Injectable and porous PLGA microspheres that form highly porous scaffolds at body temperature. Acta Biomater 10(12):5090–5098. https://doi.org/10.1016/j.actbio.2014.08.015
44. Flégeau K, Puiggali-Jou A, Zenobi-Wong M (2022) Cartilage tissue engineering by extrusion bioprinting utilizing porous hyaluronic acid microgel bioinks. Biofabrication 14(3):034105. https://doi.org/10.1088/1758-5090/ac6b58
45. Mostafavi A, Samandari M, Karvar M et al (2021) Colloidal

multiscale porous adhesive (bio)inks facilitate scaffold integration. Appl Phys Rev 8(4):041415. https://doi.org/10.1063/5.0062823
46. Luo ZY, Tang GS, Ravanbakhsh H et al (2022) Vertical extrusion cryo(bio)printing for anisotropic tissue manufacturing. Adv Mater 34(12):e2108931. https://doi.org/10.1002/adma.202108931
47. Bao GY, Jiang T, Ravanbakhsh H et al (2020) Triggered micropore-forming bioprinting of porous viscoelastic hydrogels. Mater Horiz 7(9):2336–2347. https://doi.org/10.1039/D0MH00813C
48. Kim WJ, Kim GH (2022) Highly bioactive cell-laden hydrogel constructs bioprinted using an emulsion bioink for tissue engineering applications. Biofabrication 14(4):045018. https://doi.org/10.1088/1758-5090/ac8fb8
49. Ying GL, Jiang N, Maharjan S et al (2018) Aqueous two-phase emulsion bioink-enabled 3D bioprinting of porous hydrogels. Adv Mater 30(50):1805460. https://doi.org/10.1002/adma.201805460
50. Ouyang L, Armstrong JPK, Chen Q et al (2020) Void-free 3D bioprinting for in situ endothelialization and microfluidic perfusion. Adv Funct Mater 30(1):1908349. https://doi.org/10.1002/adfm.201908349
51. Mironov V, Visconti RP, Kasyanov V et al (2009) Organ printing: tissue spheroids as building blocks. Biomaterials 30(12): 2164–2174. https://doi.org/10.1016/j.biomaterials.2008.12.084
52. Tan YJ, Tan XP, Yeong WY et al (2016) Hybrid microscaffold-based 3D bioprinting of multi-cellular constructs with high compressive strength: a new biofabrication strategy. Sci Rep 6:39140. https://doi.org/10.1038/srep39140
53. Norotte C, Marga FS, Niklason LE et al (2009) Scaffold-free vascular tissue engineering using bioprinting. Biomaterials 30(30): 5910–5917. https://doi.org/10.1016/j.biomaterials.2009.06.034
54. Zhu W, Ma XY, Gou ML et al (2016) 3D printing of functional biomaterials for tissue engineering. Curr Opin Biotechnol 40:103–112. https://doi.org/10.1016/j.copbio.2016.03.014
55. Hwang HH, Zhu W, Victorine G et al (2018) 3D-printing of functional biomedical microdevices via light- and extrusion-based approaches. Small Meth 2(2):1700277. https://doi.org/10.1002/smtd.201700277
56. You ST, Li JW, Zhu W et al (2018) Nanoscale 3D printing of hydrogels for cellular tissue engineering. J Mater Chem B 6(15): 2187–2197. https://doi.org/10.1039/C8TB00301G
57. You ST, Zhu W, Wang PR et al (2019) Projection printing of ultrathin structures with nanoscale thickness control. ACS Appl Mater Interfaces 11(17):16059–16064. https://doi.org/10.1021/acsami.9b02728
58. You ST, Xiang Y, Hwang HH et al (2023) High cell density and high-resolution 3D bioprinting for fabricating vascularized tissues. Sci Adv 9(8):eade7923. https://doi.org/10.1126/sciadv.ade7923
59. Zhang JH, Xin W, Qin YC et al (2022) "All-in-one" zwitterionic granular hydrogel bioink for stem cell spheroids production and 3D bioprinting. Chem Eng J 430:132713. https://doi.org/10.1016/j.cej.2021.132713
60. Deo KA, Murali A, Tronolone JJ et al (2024) Granular biphasic colloidal hydrogels for 3D bioprinting. Adv Healthc Mater 13(25): e2303810. https://doi.org/10.1002/adhm.202303810
61. Truong NF, Kurt E, Tahmizyan N et al (2019) Microporous annealed particle hydrogel stiffness, void space size, and adhesion properties impact cell proliferation, cell spreading, and gene transfer. Acta Biomater 94:160–172. https://doi.org/10.1016/j.actbio.2019.02.054
62. Griffin DR, Weaver WM, Scumpia PO et al (2015) Accelerated wound healing by injectable microporous gel scaffolds assembled from annealed building blocks. Nat Mater 14(7):737–744. https://doi.org/10.1038/nmat4294
63. Li FY, Levinson C, Truong VX et al (2020) Microencapsulation improves chondrogenesis in vitro and cartilaginous matrix stability in vivo compared to bulk encapsulation. Biomater Sci 8(6): 1711–1725. https://doi.org/10.1039/C9BM01524H
64. Puiggalí-Jou A, Asadikorayem M, Maniura-Weber K et al (2023) Growth factor–loaded sulfated microislands in granular hydrogels promote hMSCs migration and chondrogenic differentiation. Acta Biomater 166:69–84. https://doi.org/10.1016/j.actbio.2023.03.045
65. Muir VG, Qazi TH, Weintraub S et al (2022) Sticking together: injectable granular hydrogels with increased functionality via dynamic covalent inter-particle crosslinking. Small 18(36):2201115. https://doi.org/10.1002/smll.202201115
66. Morley CD, Tordoff J, O'Bryan CS et al (2020) 3D aggregation of cells in packed microgel media. Soft Matter 16(28):6572–6581. https://doi.org/10.1039/D0SM00517G
67. Ataie Z, Kheirabadi S, Zhang JW et al (2022) Nanoengineered granular hydrogel bioinks with preserved interconnected microporosity for extrusion bioprinting. Small 18(37):2202390. https://doi.org/10.1002/smll.202202390
68. de Rutte JM, Koh J, Carlo DD (2019) Scalable high-throughput production of modular microgels for in situ assembly of microporous tissue scaffolds. Adv Funct Mater 29(25):1900071. https://doi.org/10.1002/adfm.201900071
69. Béduer A, Piacentini N, Aeberli L et al (2018) Additive manufacturing of hierarchical injectable scaffolds for tissue engineering. Acta Biomater 76:71–79. https://doi.org/10.1016/j.actbio.2018.05.056
70. Castilho M, Levato R, Bernal PN et al (2021) Hydrogel-based bioinks for cell electrowriting of well-organized living structures with micrometer-scale resolution. Biomacromolecules 22(2): 855–866. https://doi.org/10.1021/acs.biomac.0c01577
71. Kessel B, Lee M, Bonato A et al (2020) 3D bioprinting of macroporous materials based on entangled hydrogel microstrands. Adv Sci 7(18):2001419. https://doi.org/10.1002/advs.202001419
72. Ji CD, Annabi N, Khademhosseini A et al (2011) Fabrication of porous chitosan scaffolds for soft tissue engineering using dense gas CO_2. Acta Biomater 7(4):1653–1664. https://doi.org/10.1016/j.actbio.2010.11.043
73. Weber P, Cai L, Rojas FJA et al (2024) Microfluidic bubble-generator enables digital light processing 3D printing of porous structures. Aggregate 5(1):e409. https://doi.org/10.1002/agt2.409
74. Koo YW, Lee H, Lim CS et al (2022) Highly porous multiple-cell-laden collagen/hydroxyapatite scaffolds for bone tissue engineering. Int J Biol Macromol 222:1264–1276. https://doi.org/10.1016/j.ijbiomac.2022.09.249
75. Koo YW, Kim GH (2022) Bioprinted hASC-laden collagen/HA constructs with meringue-like macro/micropores. Bioeng Transl Med 7(3):e10330. https://doi.org/10.1002/btm2.10330
76. Mainardi JC, Demarchi CB, Mirdrikvand M et al (2022) 3D

bioprinting of hydrogel/ceramic composites with hierarchical porosity. J Mater Sci 57(5):3662–3677. https://doi.org/10.1007/s10853-021-06829-7
77. Zhai X, Chen WW (2019) Compressive mechanical response of porcine muscle at intermediate (10^0/s-10^2/s) strain rates. Exp Mech 59(9):1299–1305. https://doi.org/10.1007/s11340-018-00456-1
78. Woodard JR, Hilldore AJ, Lan SK et al (2007) The mechanical properties and osteoconductivity of hydroxyapatite bone scaffolds with multi-scale porosity. Biomaterials 28(1):45–54. https://doi.org/10.1016/j.biomaterials.2006.08.021
79. Ying GL, Jiang N, Parra-Cantu C et al (2020) Bioprinted injectable hierarchically porous gelatin methacryloyl hydrogel constructs with shape-memory properties. Adv Funct Mater 30(46):2003740. https://doi.org/10.1002/adfm.202003740
80. Janarthanan G, Kim JH, Kim I et al (2022) Manufacturing of self-standing multi-layered 3D-bioprinted alginate-hyaluronate constructs by controlling the cross-linking mechanisms for tissue engineering applications. Biofabrication 14(3):035013. https://doi.org/10.1088/1758-5090/ac6c4c
81. Zhu MF, Li W, Dong XH et al (2019) In vivo engineered extracellular matrix scaffolds with instructive niches for oriented tissue regeneration. Nat Commun 10:4620. https://doi.org/10.1038/s41467-019-12545-3
82. Adamkiewicz M, Rubinsky B (2015) Cryogenic 3D printing for tissue engineering. Cryobiology 71(3):518–521. https://doi.org/10.1016/j.cryobiol.2015.10.152
83. Zhang WC, Ullah I, Shi L et al (2019) Fabrication and characterization of porous polycaprolactone scaffold via extrusion-based cryogenic 3D printing for tissue engineering. Mater Des 180:107946. https://doi.org/10.1016/j.matdes.2019.107946
84. Wu CX, Yu ZH, Li YH et al (2020) Cryogenically printed flexible chitosan/bioglass scaffolds with stable and hierarchical porous structures for wound healing. Biomed Mater 16(1):015004. https://doi.org/10.1088/1748-605x/abb2d7
85. Sobral JM, Caridade SG, Sousa RA et al (2011) Three-dimensional plotted scaffolds with controlled pore size gradients: effect of scaffold geometry on mechanical performance and cell seeding efficiency. Acta Biomater 7(3):1009–1018. https://doi.org/10.1016/j.actbio.2010.11.003
86. Hu B, Li GK, Ai GM et al (2022) Macrocycle molecule-based cryoprotectants for ice recrystallization inhibition and cell cryopreservation. J Mater Chem B 10(36):6922–6927. https://doi.org/10.1039/D2TB01083F
87. Guerreiro BM, Concórdio-Reis P, Pericão H et al (2024) Elevated fucose content enhances the cryoprotective performance of anionic polysaccharides. Int J Biol Macromol 261:129577. https://doi.org/10.1016/j.ijbiomac.2024.129577
88. Luo ZY, Lian LM, Stocco T et al (2024) 3D assembly of cryo(bio)printed modular units for shelf-ready scalable tissue fabrication. Adv Funct Mater 34(4):2309173. https://doi.org/10.1002/adfm.202309173
89. Malda J, Visser J, Melchels FP et al (2013) 25th anniversary article: engineering hydrogels for biofabrication. Adv Mater 25(36): 5011–5028. https://doi.org/10.1002/adma.201302042
90. Monette A, Ceccaldi C, Assaad E et al (2016) Chitosan thermogels for local expansion and delivery of tumor-specific T lymphocytes towards enhanced cancer immunotherapies. Biomaterials 75:237–249. https://doi.org/10.1016/j.biomaterials.2015.10.021
91. Dong ZQ, Cui HJ, Zhang HD et al (2021) 3D printing of inherently nanoporous polymers via polymerization-induced phase separation. Nat Commun 12:247. https://doi.org/10.1038/s41467-020-20498-1
92. Wu JL, Xu F, Li SM et al (2019) Porous polymers as multifunctional material platforms toward task-specific applications. Adv Mater 31(4):1802922. https://doi.org/10.1002/adma.201802922
93. Bobrin VA, Yao Y, Shi XB et al (2022) Nano- to macro-scale control of 3D printed materials via polymerization induced microphase separation. Nat Commun 13:3577. https://doi.org/10.1038/s41467-022-31095-9
94. Ouyang LL, Yao R, Zhao Y et al (2016) Effect of bioink properties on printability and cell viability for 3D bioplotting of embryonic stem cells. Biofabrication 8(3):035020. https://doi.org/10.1088/1758-5090/8/3/035020
95. Chaudhuri O, Gu L, Klumpers D et al (2016) Hydrogels with tunable stress relaxation regulate stem cell fate and activity. Nat Mater 15(3):326–334. https://doi.org/10.1038/nmat4489
96. Wan Y, Wang R, Feng W et al (2021) High internal phase Pickering emulsions stabilized by co-assembled rice proteins and carboxymethyl cellulose for food-grade 3D printing. Carbohydr Polym 273:118586. https://doi.org/10.1016/j.carbpol.2021.118586
97. Ma T, Cui RR, Lu SY et al (2022) High internal phase Pickering emulsions stabilized by cellulose nanocrystals for 3D printing. Food Hydrocoll 125:107418. https://doi.org/10.1016/j.foodhyd.2021.107418
98. Zong YC, Kuang Q, Liu GJ et al (2022) All-natural protein-polysaccharide conjugates with bead-on-a-string nanostructures as stabilizers of high internal phase emulsions for 3D printing. Food Chem 388:133012. https://doi.org/10.1016/j.foodchem.2022.133012
99. Wang QB, Karadas Ö, Backman O et al (2023) Aqueous two-phase emulsion bioresin for facile one-step 3D microgel-based bioprinting. Adv Healthc Mater 12(19):2203243. https://doi.org/10.1002/adhm.202203243
100. Tao J, Zhu SY, Liao XY et al (2022) DLP-based bioprinting of void-forming hydrogels for enhanced stem-cell-mediated bone regeneration. Mater Today Bio 17:100487. https://doi.org/10.1016/j.mtbio.2022.100487
101. Jia LT, Hua YJ, Zeng JS et al (2022) Bioprinting and regeneration of auricular cartilage using a bioactive bioink based on microporous photocrosslinkable acellular cartilage matrix. Bioact Mater 16:66–81. https://doi.org/10.1016/j.bioactmat.2022.02.032
102. Zhang X, Liu Y, Luo CY et al (2021) Crosslinker-free silk/decellularized extracellular matrix porous bioink for 3D bioprinting-based cartilage tissue engineering. Mater Sci Eng C 118:111388. https://doi.org/10.1016/j.msec.2020.111388
103. Ng WL, Goh MH, Yeong WY et al (2018) Applying macromolecular crowding to 3D bioprinting: fabrication of 3D hierarchical porous collagen-based hydrogel constructs. Biomater Sci 6(3): 562–574. https://doi.org/10.1039/C7BM01015J
104. Qin XS, Wang M, Li WL et al (2022) Biosurfactant-stabilized micropore-forming GelMA inks enable improved usability for 3D printing applications. Regen Eng Transl Med 8:471-481. https://doi.org/10.1007/s40883-022-00250-5
105. Hu QP, Liu X, Liu HF et al (2021) 3D printed porous microgel for lung cancer cells culture in vitro. Mater Des 210:110079. https://doi.org/10.1016/j.matdes.2021.110079
106. Shao L, Hou RX, Zhu YB et al (2021) Pre-shear bioprinting of

highly oriented porous hydrogel microfibers to construct anisotropic tissues. Biomater Sci 9(20):6763–6771. https://doi.org/10.1039/D1BM00695A
107. Ying G, Manríquez J, Wu D et al (2020) An open-source handheld extruder loaded with pore-forming bioink for in situ wound dressing. Mater Today Bio 8:100074. https://doi.org/10.1016/j.mtbio.2020.100074
108. Tao J, Zhu SY, Zhou NZ et al (2022) Nanoparticle-stabilized emulsion bioink for digital light processing based 3D bioprinting of porous tissue constructs. Adv Healthc Mater 11(12):2102810. https://doi.org/10.1002/adhm.202102810
109. Wang M, Li WL, Luo ZY et al (2022) A multifunctional micropore-forming bioink with enhanced anti-bacterial and anti-inflammatory properties. Biofabrication 14(2):024105. https://doi.org/10.1088/1758-5090/ac5936
110. Yi SL, Liu Q, Luo ZY et al (2022) Micropore-forming gelatin methacryloyl (GelMA) bioink toolbox 2.0: designable tunability and adaptability for 3D bioprinting applications. Small 18(25): 2106357. https://doi.org/10.1002/smll.202106357
111. Sears NA, Wilems TS, Gold KA et al (2019) Hydrocolloid inks for 3D printing of porous hydrogels. Adv Mater Technol 4(2): 1800343. https://doi.org/10.1002/admt.201800343
112. Cabezas H (1996) Theory of phase formation in aqueous two-phase systems. J Chromatogr B Biomed Sci Appl 680(1–2):3–30. https://doi.org/10.1016/0378-4347(96)00042-4
113. Levato R, Lim KS, Li WL et al (2021) High-resolution lithographic biofabrication of hydrogels with complex microchannels from low-temperature-soluble gelatin bioresins. Mater Today Bio 12:100162. https://doi.org/10.1016/j.mtbio.2021.100162
114. Messaoud GB, Aveic S, Wachendoerfer M et al (2023) 3D printable gelatin methacryloyl (GelMA)-dextran aqueous two-phase system with tunable pores structure and size enables physiological behavior of embedded cells in vitro. Small 19(44):e2208089. https://doi.org/10.1002/smll.202208089
115. Gonzalez-Fernandez T, Rathan S, Hobbs C et al (2019) Pore-forming bioinks to enable spatio-temporally defined gene delivery in bioprinted tissues. J Control Release 301:13–27. https://doi.org/10.1016/j.jconrel.2019.03.006
116. Armstrong JPK, Burke M, Carter BM et al (2016) 3D bioprinting using a templated porous bioink. Adv Healthc Mater 5(14): 1724–1730. https://doi.org/10.1002/adhm.201600022
117. Ouyang LL, Wojciechowski JP, Tang JQ et al (2022) Tunable microgel-templated porogel (MTP) bioink for 3D bioprinting applications. Adv Healthc Mater 11(8):2200027. https://doi.org/10.1002/adhm.202200027
118. Zou Q, Grottkau BE, He ZX et al (2020) Biofabrication of valentine-shaped heart with a composite hydrogel and sacrificial material. Mater Sci Eng C Mater Biol Appl 108:110205. https://doi.org/10.1016/j.msec.2019.110205
119. Xu F, Sridharan BP, Durmus NG et al (2011) Living bacterial sacrificial porogens to engineer decellularized porous scaffolds. PLoS ONE 6(4):e19344. https://doi.org/10.1371/journal.pone.0019344
120. Jeon O, Lee YB, Hinton TJ et al (2019) Cryopreserved cell-laden alginate microgel bioink for 3D bioprinting of living tissues. Mater Today Chem 12:61–70. https://doi.org/10.1016/j.mtchem.2018.11.009
121. Shao L, Gao Q, Xie CQ et al (2020) Sacrificial microgel-laden bioink-enabled 3D bioprinting of mesoscale pore networks. Bio-Des Manuf 3(1):30–39. https://doi.org/10.1007/s42242-020-00062-y
122. Seymour AJ, Shin S, Heilshorn SC (2021) 3D printing of microgel scaffolds with tunable void fraction to promote cell infiltration. Adv Healthc Mater 10(18):e2100644. https://doi.org/10.1002/adhm.202100644
123. Ouyang LL, Highley CB, Rodell CB et al (2016) 3D printing of shear-thinning hyaluronic acid hydrogels with secondary cross-linking. ACS Biomater Sci Eng 2(10):1743–1751. https://doi.org/10.1021/acsbiomaterials.6b00158
124. Hidalgo C, Méndez-Ruette M, Zavala G et al (2023) A novel porous hydrogel based on hybrid gelation for injectable and tough scaffold implantation and tissue engineering applications. Biomed Mater 18(4):045014. https://doi.org/10.1088/1748-605X/acd499
125. Zhou Y, Fan YC, Chen Z et al (2022) Catechol functionalized ink system and thrombin-free fibrin gel for fabricating cellular constructs with mechanical support and inner micro channels. Biofabrication 14(1):015004. https://doi.org/10.1088/1758-5090/ac2ef8
126. Xie MJ, Sun Y, Wang J et al (2022) Thermo-sensitive sacrificial microsphere-based bioink for centimeter-scale tissue with angiogenesis. Int J Bioprinting 8(4):599. https://doi.org/10.18063/ijb.v8i4.599
127. Shen MK, Wang LL, Gao Y et al (2022) 3D bioprinting of in situ vascularized tissue engineered bone for repairing large segmental bone defects. Mater Today Bio 16:100382. https://doi.org/10.1016/j.mtbio.2022.100382
128. Ching T, Vasudevan J, Chang SY et al (2022) Biomimetic vasculatures by 3D-printed porous molds. Small 18(39):2203426. https://doi.org/10.1002/smll.202203426
129. Enrico A, Voulgaris D, Östmans R et al (2022) 3D microvascularized tissue models by laser-based cavitation molding of collagen. Adv Mater 34(11):2109823. https://doi.org/10.1002/adma.202109823
130. Lewis MC, MacArthur BD, Malda J et al (2005) Heterogeneous proliferation within engineered cartilaginous tissue: the role of oxygen tension. Biotechnol Bioeng 91(5):607–615. https://doi.org/10.1002/bit.20508
131. Kolesky DB, Homan KA, Skylar-Scott MA et al (2016) Three-dimensional bioprinting of thick vascularized tissues. Proc Natl Acad Sci USA 113(12):3179–3184. https://doi.org/10.1073/pnas.1521342113
132. Lode A, Krujatz F, Brüggemeier S et al (2015) Green bioprinting: fabrication of photosynthetic algae-laden hydrogel scaffolds for biotechnological and medical applications. Eng Life Sci 15(2): 177–183. https://doi.org/10.1002/elsc.201400205
133. Maharjan S, Alva J, Cámara C et al (2021) Symbiotic photosynthetic oxygenation within 3D-bioprinted vascularized tissues. Matter 4(1):217–240. https://doi.org/10.1016/j.matt.2020.10.022
134. Chu LY, Jiang GQ, Hu XL et al (2018) Biodegradable macroporous scaffold with nano-crystal surface microstructure for highly effective osteogenesis and vascularization. J Mater Chem B 6(11): 1658–1667. https://doi.org/10.1039/C7TB03353B
135. Wei XY, Luo YX, Huang P (2019) 3D bioprinting of alginate scaffolds with controlled micropores by leaching of recrystallized salts. Polym Bull 76(12):6077–6088. https://doi.org/10.1007/s00289-019-02690-6
136. Zhang L, Tang H, Xiahou ZJ et al (2022) Solid multifunctional granular bioink for constructing chondroid basing on stem cell

spheroids and chondrocytes. Biofabrication 14(3):035003. https://doi.org/10.1088/1758-5090/ac63ee
137. Hirano M, Huang YK, Jarquin DV et al (2021) 3D bioprinted human iPSC-derived somatosensory constructs with functional and highly purified sensory neuron networks. Biofabrication 13(3):035046. https://doi.org/10.1088/1758-5090/abff11
138. Fan CJ, Ling Y, Deng WS et al (2019) A novel cell encapsulatable cryogel (CECG) with macro-porous structures and high permeability: a three-dimensional cell culture scaffold for enhanced cell adhesion and proliferation. Biomed Mater 14(5):055006. https://doi.org/10.1088/1748-605X/ab2efd
139. Ambekar RS, Kandasubramanian B (2019) Progress in the advancement of porous biopolymer scaffold: tissue engineering application. Ind Eng Chem Res 58(16):6163–6194. https://doi.org/10.1021/acs.iecr.8b05334
140. Bae H, Puranik AS, Gauvin R et al (2012) Building vascular networks. Sci Transl Med 4(160):160ps23. https://doi.org/10.1126/scitranslmed.3003688
141. Zhang YS, Khademhosseini A (2015) Seeking the right context for evaluating nanomedicine: from tissue models in Petri dishes to microfluidic organs-on-a-chip. Nanomedicine 10(5):685–688. https://doi.org/10.2217/nnm.15.18
142. Heinrich MA, Liu WJ, Jimenez A et al (2019) 3D bioprinting: from benches to translational applications. Small 15(23):1805510. https://doi.org/10.1002/smll.201805510
143. Lee VK, Kim DY, Ngo H et al (2014) Creating perfused functional vascular channels using 3D bio-printing technology. Biomaterials 35(28):8092–8102. https://doi.org/10.1016/j.biomaterials.2014.05.083
144. Miller JS, Stevens KR, Yang MT et al (2012) Rapid casting of patterned vascular networks for perfusable engineered three-dimensional tissues. Nat Mater 11(9):768–774. https://doi.org/10.1038/nmat3357
145. Gupta D, Singh AK, Dravid A et al (2019) Multiscale porosity in compressible cryogenically 3D printed gels for bone tissue engineering. ACS Appl Mater Interfaces 11(22):20437–20452. https://doi.org/10.1021/acsami.9b05460
146. Roosa SMM, Kemppainen JM, Moffitt EN et al (2010) The pore size of polycaprolactone scaffolds has limited influence on bone regeneration in an in vivo model. J Biomed Mater Res Part A 92A(1):359–368. https://doi.org/10.1002/jbm.a.32381
147. Owen R, Sherborne C, Paterson T et al (2016) Emulsion templated scaffolds with tunable mechanical properties for bone tissue engineering. J Mech Behav Biomed Mater 54:159–172. https://doi.org/10.1016/j.jmbbm.2015.09.019
148. Cameron NR, Sherrington DC, Albiston L et al (1996) Study of the formation of the open-cellular morphology of poly(styrene/divinylbenzene) polyHIPE materials by cryo-SEM. Colloid Polym Sci 274(6):592–595. https://doi.org/10.1007/BF00655236
149. Wang M, Li WL, Mille LS et al (2022) Digital light processing based bioprinting with composable gradients. Adv Mater 34(1):2107038. https://doi.org/10.1002/adma.202107038
150. Sengokmen-Ozsoz N, Aleemardani M, Palanca M et al (2025) Fabrication of hierarchically porous trabecular bone replicas via 3D printing with high internal phase emulsions (HIPEs). Biofabrication 17(1):015012. https://doi.org/10.1088/1758-5090/ad8b70
151. Du SR, Huynh T, Lu YZ et al (2024) Bioactive polymer composite scaffolds fabricated from 3D printed negative molds enable bone formation and vascularization. Acta Biomater 186:260–274. https://doi.org/10.1016/j.actbio.2024.07.038
152. Ho CT, Lin RZ, Chen RJ et al (2013) Liver-cell patterning lab chip: mimicking the morphology of liver lobule tissue. Lab Chip 13(18):3578–3587. https://doi.org/10.1039/C3LC50402F
153. Lee JS, Cho SW (2012) Liver tissue engineering: recent advances in the development of a bio-artificial liver. Biotechnol Bioprocess Eng 17(3):427–438. https://doi.org/10.1007/s12257-012-0047-9
154. Bhise NS, Manoharan V, Massa S et al (2016) A liver-on-a-chip platform with bioprinted hepatic spheroids. Biofabrication 8(1):014101. https://doi.org/10.1088/1758-5090/8/1/014101
155. Sun GM, Zhang XJ, Shen YI et al (2011) Dextran hydrogel scaffolds enhance angiogenic responses and promote complete skin regeneration during burn wound healing. Proc Natl Acad Sci USA 108(52):20976–20981. https://doi.org/10.1073/pnas.1115973108
156. Duval C, Chagnoleau C, Pouradier F et al (2012) Human skin model containing melanocytes: essential role of keratinocyte growth factor for constitutive pigmentation-functional response to α-melanocyte stimulating hormone and forskolin. Tissue Eng Part C Methods 18(12):947–957. https://doi.org/10.1089/ten.tec.2011.0676
157. Ng WL, Qi JTZ, Yeong WY et al (2018) Proof-of-concept: 3D bioprinting of pigmented human skin constructs. Biofabrication 10(2):025005. https://doi.org/10.1088/1758-5090/aa9e1e[PubMDed]
158. Heng MCY (2011) Wound healing in adult skin: aiming for perfect regeneration. Int J Dermatol 50(9):1058–1066. https://doi.org/10.1111/j.1365-4632.2011.04940.x
159. Zhou FF, Hong Y, Liang RJ et al (2020) Rapid printing of bio-inspired 3D tissue constructs for skin regeneration. Biomaterials 258:120287. https://doi.org/10.1016/j.biomaterials.2020.120287
160. Dejob L, Toury B, Tadier S et al (2021) Electrospinning of in situ synthesized silica-based and calcium phosphate bioceramics for applications in bone tissue engineering: a review. Acta Biomater 123:123–153. https://doi.org/10.1016/j.actbio.2020.12.032
161. Koons GL, Diba M, Mikos AG (2020) Materials design for bone-tissue engineering. Nat Rev Mater 5(8):584–603. https://doi.org/10.1038/s41578-020-0204-2
162. Liu XZ, Chen MM, Luo JC et al (2021) Immunopolarization-regulated 3D printed-electrospun fibrous scaffolds for bone regeneration. Biomaterials 276:121037. https://doi.org/10.1016/j.biomaterials.2021.121037
163. Shang FQ, Yu Y, Liu SY et al (2021) Advancing application of mesenchymal stem cell-based bone tissue regeneration. Bioact Mater 6(3):666–683. https://doi.org/10.1016/j.bioactmat.2020.08.014
164. Loebel C, Burdick JA (2018) Engineering stem and stromal cell therapies for musculoskeletal tissue repair. Cell Stem Cell 22(3):325–339. https://doi.org/10.1016/j.stem.2018.01.014
165. Clark AY, Martin KE, García JR et al (2020) Integrin-specific hydrogels modulate transplanted human bone marrow-derived mesenchymal stem cell survival, engraftment, and reparative activities. Nat Commun 11:114. https://doi.org/10.1038/s41467-019-14000-9
166. Liu Y, Li T, Sun ML et al (2022) ZIF-8 modified multifunctional injectable photopolymerizable GelMA hydrogel for the treatment of periodontitis. Acta Biomater 146:37–48.

https://doi.org/10.1016/j.actbio.2022.03.046
167. Zhao X, Liu S, Yildirimer L et al (2016) Injectable stem cell-laden photocrosslinkable microspheres fabricated using microfluidics for rapid generation of osteogenic tissue constructs. Adv Funct Mater 26(17):2809–2819. https://doi.org/10.1002/adfm.201504943
168. Turnbull G, Clarke J, Picard F et al (2018) 3D bioactive composite scaffolds for bone tissue engineering. Bioact Mater 3(3):278–314. https://doi.org/10.1016/j.bioactmat.2017.10.001
169. Jain P, Kathuria H, Dubey N (2022) Advances in 3D bioprinting of tissues/organs for regenerative medicine and in-vitro models. Biomaterials 287:121639. https://doi.org/10.1016/j.biomaterials.2022.121639
170. Jo Y, Hwang DG, Kim M et al (2023) Bioprinting-assisted tissue assembly to generate organ substitutes at scale. Trends Biotechnol 41(1):93–105. https://doi.org/10.1016/j.tibtech.2022.07.001
171. Zhang M, Lin RC, Wang X et al (2020) 3D printing of Haversian bone-mimicking scaffolds for multicellular delivery in bone regeneration. Sci Adv 6(12):eaaz6725. https://doi.org/10.1126/sciadv.aaz6725
172. Cui XF, Breitenkamp K, Finn MG et al (2012) Direct human cartilage repair using three-dimensional bioprinting technology. Tissue Eng Part A 18(11–12):1304–1312. https://doi.org/10.1089/ten.TEA.2011.0543
173. Schuurman W, Levett PA, Pot MW et al (2013) Gelatin-methacrylamide hydrogels as potential biomaterials for fabrication of tissue-engineered cartilage constructs. Macromol Biosci 13(5):551–561. https://doi.org/10.1002/mabi.201200471
174. Markstedt K, Mantas A, Tournier I et al (2015) 3D bioprinting human chondrocytes with nanocellulose-alginate bioink for cartilage tissue engineering applications. Biomacromolecules 16(5):1489–1496. https://doi.org/10.1021/acs.biomac.5b00188
175. Hwang CM, Lee BK, Green D et al (2014) Auricular reconstruction using tissue-engineered alloplastic implants for improved clinical outcomes. Plast Reconstr Surg 133(3):360e–369e. https://doi.org/10.1097/01.prs.0000438460.68098.4b
176. Bolívar-Monsalve EJ, Ceballos-González CF, Chávez-Madero C et al (2022) One-step bioprinting of multi-channel hydrogel filaments using chaotic advection: fabrication of pre-vascularized muscle-like tissues. Adv Healthc Mater 11:2200448. https://doi.org/10.1002/adhm.202200448
177. Bova L, Maggiotto F, Micheli S et al (2023) A porous gelatin methacrylate-based material for 3D cell-laden constructs. Macromol Biosci 23(2):e2200357. https://doi.org/10.1002/mabi.202200357
178. Feng ZY, Su X, Wang T et al (2023) The role of microsphere structures in bottom-up bone tissue engineering. Pharmaceutics 15(2):321. https://doi.org/10.3390/pharmaceutics15020321
179. Jayachandran V, Murugan SS, Dalavi PA et al (2022) Alginate-based composite microspheres: preparations and applications for bone tissue engineering. Curr Pharm Des 28(13):1067–1081. https://doi.org/10.2174/1381612828666220518142911
180. Pan Q, Su WX, Yao YC (2023) Progress in microsphere-based scaffolds in bone/cartilage tissue engineering. Biomed Mater 18(6):062004. https://doi.org/10.1088/1748-605X/acfd78
181. Zhao XB, Zhou YY, Li JT et al (2022) Opportunities and challenges of hydrogel microspheres for tendon–bone healing after anterior cruciate ligament reconstruction. J Biomed Mater Res Part B Appl Biomater 110(2):289–301. https://doi.org/10.1002/jbm.b.34925
182. Boas FE, Bodei L, Sofocleous CT (2017) Radioembolization of colorectal liver metastases: indications, technique, and outcomes. J Nucl Med 58(suppl 2):104S–111S. https://doi.org/10.2967/jnumed.116.187229
183. Kim HC (2017) Radioembolization for the treatment of hepatocellular carcinoma. Clin Mol Hepatol 23(2):109–114. https://doi.org/10.3350/cmh.2017.0004
184. Liaw CY, Ji S, Guvendiren M (2018) Engineering 3D hydrogels for personalized in vitro human tissue models. Adv Healthc Mater 7(4):1701165. https://doi.org/10.1002/adhm.201701165
185. Townsend AR, Chong LC, Karapetis C et al (2016) Selective internal radiation therapy for liver metastases from colorectal cancer. Cancer Treat Rev 50:148–154. https://doi.org/10.1016/j.ctrv.2016.09.007
186. Negro A, Cherbuin T, Lutolf MP (2018) 3D inkjet printing of complex, cell-laden hydrogel structures. Sci Rep 8(1):17099. https://doi.org/10.1038/s41598-018-35504-2
187. Khalighi S, Saadatmand M (2021) Bioprinting a thick and cell-laden partially oxidized alginate-gelatin scaffold with embedded micro-channels as future soft tissue platform. Int J Biol Macromol 193:2153–2164. https://doi.org/10.1016/j.ijbiomac.2021.11.046
188. Wang Y, Delarue AP, McAninch IM et al (2022) Digital light processing of highly filled polymer composites with interface-mediated mechanical properties. ACS Appl Polym Mater 4(9):6477–6486. https://doi.org/10.1021/acsapm.2c00890
189. Barradas AM, Yuan HP, van Blitterswijk CA et al (2011) Osteoinductive biomaterials: current knowledge of properties, experimental models and biological mechanisms. Eur Cell Mater 21:407–429. https://doi.org/10.22203/ecm.v021a31
190. Tao J, Xu X, Wang S et al (2019) Polydiacetylene-nanoparticle-functionalized microgels for topical bacterial infection treatment. ACS Macro Lett 8(5):563–568. https://doi.org/10.1021/acsmacrolett.9b00196
191. Shao L, Gao Q, Xie CQ et al (2020) Directly coaxial 3D bioprinting of large-scale vascularized tissue constructs. Biofabrication 12(3):035014. https://doi.org/10.1088/1758-5090/ab7e76
192. Zhou X, Nowicki M, Sun H et al (2020) 3D bioprinting-tunable small-diameter blood vessels with biomimetic biphasic cell layers. ACS Appl Mater Interfaces 12(41):45904–45915. https://doi.org/10.1021/acsami.0c14871
193. Zhao GX, Zhou HW, Jin GR et al (2022) Rational design of electrically conductive biomaterials toward excitable tissues regeneration. Prog Polym Sci 131:101573. https://doi.org/10.1016/j.progpolymsci.2022.101573
194. Jiang ZY, Song Q, Tang ML et al (2016) Enhanced migration of neural stem cells by microglia grown on a three-dimensional graphene scaffold. ACS Appl Mater Interfaces 8(38):25069–25077. https://doi.org/10.1021/acsami.6b06780
195. Ma QQ, Yang LY, Jiang ZY et al (2016) Three-dimensional stiff graphene scaffold on neural stem cells behavior. ACS Appl Mater Interfaces 8(50):34227–34233. https://doi.org/10.1021/acsami.6b12305
196. Wang J, Wang HY, Mo XM et al (2020) Reduced graphene oxide-encapsulated microfiber patterns enable controllable formation of neuronal-like networks. Adv Mater 32(40):2004555. https://doi.org/10.1002/adma.202004555
197. Wu W, DeConinck A, Lewis JA (2011) Omnidirectional printing

of 3D microvascular networks. Adv Mater 23(24):H178–H183. https://doi.org/10.1002/adma.201004625
198. Wang HY, Zhou XQ, Wang J et al (2022) Fabrication of channeled scaffolds through polyelectrolyte complex (PEC) printed sacrificial templates for tissue formation. Bioact Mater 17:261–275. https://doi.org/10.1016/j.bioactmat.2022.01.030
199. Costantini M, Colosi C, Święszkowski W et al (2019) Co-axial wet-spinning in 3D bioprinting: state of the art and future perspective of microfluidic integration. Biofabrication 11(1):012001. https://doi.org/10.1088/1758-5090/aae605
200. Tang GS, Luo ZY, Lian LM et al (2023) Liquid-embedded (bio)printing of alginate-free, standalone, ultrafine, and ultrathin-walled cannular structures. Proc Natl Acad Sci USA 120(7): e2206762120. https://doi.org/10.1073/pnas.2206762120
201. Xie MJ, Jin SX, Yu K et al (2024) Minimally invasive soft tissue repair using shrunken scaffolds. Nat Commun 15:6739. https://doi.org/10.1038/s41467-024-51248-2
202. Gong JX, Schuurmans CCL, van Genderen AM et al (2020) Complexation-induced resolution enhancement of 3D-printed hydrogel constructs. Nat Commun 11:1267. https://doi.org/10.1038/s41467-020-14997-4
203. Li L, Liu HF, Zhao YC et al (2024) 3D printing of maturable tissue constructs using a cell-adaptable nanocolloidal hydrogel. Adv Funct Mater 34(28):2402341. https://doi.org/10.1002/adfm.202402341
204. Willson K, Atala A (2022) Medical 3D printing: tools and techniques, today and tomorrow. Annu Rev Chem Biomol Eng 13: 481–499. https://doi.org/10.1146/annurev-chembioeng-092220-015404
205. Kuang X, Rong QZ, Belal S et al (2023) Self-enhancing sonoinks enable deep-penetration acoustic volumetric printing. Science 382(6675):1148–1155. https://doi.org/10.1126/science.adi1563
206. Zhou YF (2016) The application of ultrasound in 3D bio-printing. Molecules 21(5):590. https://doi.org/10.3390/molecules21050590
207. Xie MJ, Shi Y, Zhang C et al (2022) In situ 3D bioprinting with bioconcrete bioink. Nat Commun 13:3597. https://doi.org/10.1038/s41467-022-30997-y